Received: 4 April 2020 | Revised: 20 May 2020 | Accepted: 8 June 2020

DOI: 10.1096/fj.202000794R

RESEARCH ARTICLE

THE FASEB JOURNAL

TRPM8 as the rapid testosterone signaling receptor: Implications in the regulation of dimorphic sexual and social behaviors

Adithya Mohandass[1] | Vivek Krishnan[1] | Ekaterina D. Gribkova[2] | Swapna Asuthkar[3] | Padmamalini Baskaran[1] | Yelena Nersesyan[3] | Zahir Hussain[3,4] | Leslie M. Wise[3] | Robert E. George[3] | Nadarra Stokes[3] | Brenda M. Alexander[5] | Alejandro M. Cohen[6] | Evgeny V. Pavlov[7] | Daniel A. Llano[2] | Michael X. Zhu[8] | Baskaran Thyagarajan[1] | Eleonora Zakharian[3]

[1]College of Health Sciences, School of Pharmacy, University of Wyoming, Laramie, WY, USA

[2]Department of Molecular and Integrative Physiology, Neuroscience Program and Beckman Institute for Advanced Science and Technology, University of Illinois at Urbana Champaign, Urbana, IL, USA

[3]Department of Cancer Biology and Pharmacology, University of Illinois College of Medicine, Peoria, IL, USA

[4]Department of Physiology, Faculty of Medicine, Umm Al-Qura University, Makkah, Saudi Arabia

[5]Department of Animal Sciences, University of Wyoming, Laramie, WY, USA

[6]Biological Mass Spectrometry Core Facility, Life Sciences Research Institute, Faculty of Medicine, Dalhousie University, Halifax, NS, Canada

[7]Department of Molecular Pathobiology, New York University College of Dentistry, New York, NY, USA

[8]Department of Integrative Biology and Pharmacology, McGovern Medical School, University of Texas Health Science Center at Houston, Houston, TX, USA

Correspondence
Baskaran Thyagarajan, Molecular Signaling Laboratory, School of Pharmacy, University of Wyoming, Dept. 3375, 1000 East University Avenue, Laramie, WY 82071, USA.
Email: Baskaran.Thyagarajan@uwyo.edu

Eleonora Zakharian, Department of Cancer Biology and Pharmacology, University of Illinois, College of Medicine, 1 Illini Drive, Peoria, IL 61605, USA.
Email: zakharel@uic.edu

Funding information
National Science Foundation (NSF), Grant/Award Number: IOS-1922428; HHS | NIH | National Institute of General Medical

Abstract

Testosterone regulates dimorphic sexual behaviors in all vertebrates. However, the molecular mechanism underlying these behaviors remains unclear. Here, we report that a newly identified rapid testosterone signaling receptor, Transient Receptor Potential Melastatin 8 (TRPM8), regulates dimorphic sexual and social behaviors in mice. We found that, along with higher steroid levels in the circulation, TRPM8$^{-/-}$ male mice exhibit increased mounting frequency indiscriminate of sex, delayed sexual satiety, and increased aggression compared to wild-type controls, while TRPM8$^{-/-}$ females display an increased olfaction-exploratory behavior. Furthermore, neuronal responses to acute testosterone application onto the amygdala were attenuated in TRPM8$^{-/-}$ males but remained unchanged in females. Moreover, activation of dopaminergic neurons in the ventral tegmental area following mating was impaired in

Abbreviations: AR, androgen receptor; BSA-testosterone, bovine-serum albumin-conjugated testosterone; DA, dopaminergic neurons; DDM, dodecyl-maltoside; DHT, dihydrotestosterone; ERα, estrogen receptor α; MOS, main olfactory system; MPOA, medial preoptic area; NCB, NaCl-based buffer; OB, olfactory bulb; OE, olfactory epithelium; TH, tyrosine hydroxylase; TRPC2, transient receptor potential canonical ion channel 2; TRPM8, transient receptor potential melastatin ion channel 8; TRPV1, transient receptor potential vanilloid ion channel 1; VNO, vomeronasal organ; VTA, ventral tegmental area; WT, wild type.

Sciences (NIGMS), Grant/Award Number: 1P20GM103432-01

TRPM8$^{-/-}$ males. Together, these results demonstrate that TRPM8 regulates dimorphic sexual and social behaviors, and potentially constitutes a signalosome for mediation of sex-reward mechanism in males. Thus, deficiency of TRPM8 might lead to a delayed sexual satiety phenomenon.

KEYWORDS

aggression, dopaminergic neurons, reward system, sexual Behavior, testosterone, transient receptor potential melastatin 8 (TRPM8) channel

1 | INTRODUCTION

Sexual behavior in vertebrates presents a complex pattern of activities regulated by the central nervous and endocrine systems. Gonadal steroid hormones and their cognate receptors expressed in the brain and peripheral organ systems govern these behaviors *via* both genomic and non-genomic mechanisms.[1] Testosterone is a key steroid hormone that affects the sexual behavior and reproductive function utilizing both mechanisms. While the roles of genomic receptors in sexual behaviors are well established, molecular targets for non-genomic (rapid) actions of testosterone have only recently emerged, and are in line with increasing evidence for rapid cellular effects of steroids in the brain.[2-6] We recently discovered a novel element in rapid testosterone signaling, where the Transient Receptor Potential Melastatin 8 (TRPM8) protein acts as a highly potent ionotropic testosterone receptor.[7-10] We hypothesized that the immediate actions on the ionotropic testosterone receptor might be essential in regulating testosterone-mediated behaviors. To assess this concept, here we examined to what extent TRPM8 is involved in testosterone-dependent signaling that controls the sexual and social behaviors.

Although a connection of TRPM8 channels with any type of social or sexual behaviors has not been considered in the past, the exogenous agonist of this channel—menthol—has historically been used to increase sexual arousal, and as such has been regarded as one of "legendary chemical aphrodisiacs".[11] Menthol is known to stimulate sexual responsiveness, desire, and satisfaction.[12] Furthermore, menthol-containing formulations have been used to treat female sexual dysfunction, which was found to be more effective in female patients with significantly reduced serum levels of testosterone due to, for example, the use of oral contraceptives.[12] Revealing the linkage of testosterone actions to TRPM8 may shed light on the molecular mechanism of the menthol-elicited effects on sexual motivation and satiety.

Here, we examined the role of TRPM8 in testosterone-dependent sexual and social behaviors using sexually receptive estrous female and sexually inexperienced male mice of the wild type (WT) and TRPM8$^{-/-}$ strains, and other relative controls. Consistent with our hypothesis, we found that TRPM8$^{-/-}$ mice exhibit altered sexual behaviors, including an increased mounting frequency, delayed sexual satiety (eg, prolonged mounting activities), increased aggression, and tendency of sex-indiscriminate mating. Importantly, testosterone-induced signaling in the brain is attenuated in male, but not female, TRPM8$^{-/-}$ mice, and postmating activation of dopaminergic neurons is impaired in TRPM8$^{-/-}$ males. Together, these results not only support our original discovery that TRPM8 serves as a direct ionotropic testosterone receptor that modulates testosterone levels and steroid-dependent signaling, but also reveal a central role of this channel in the regulation of dimorphic sexual behaviors.

2 | MATERIALS AND METHODS

2.1 | Behavioral experiments

2.1.1 | Mouse behavioral testing

Adult male and female WT, TRPV1$^{-/-}$ and TRPM8$^{-/-}$ mice were purchased from Jackson Laboratory, Maine, USA, and bred in the animal house located in the School of Pharmacy University of Wyoming as per protocols approved by the IACUC. Mice were housed in a climate-controlled environment (22.8 ± 2.0°C, 45%-50% humidity) with a 12/12-light/dark cycle and access to designated diet and water ad libitum. All experiments were conducted at 22.8 ± 2.0°C. Mice once used for the tests were not used again for behavioral experiments. Estrous female mice were used for all experiments. The estrous state of females was determined as previously described.[13] All knockout strains were backcrossed with genetically unaltered WT and the heterozygotes are crossed to generate the WT and homozygotes used for the experiments.

2.1.2 | Mating Assay

Two-month-old TRPM8$^{+/+}$ (n = 16), TRPM8$^{+/-}$ (n = 8), TRPM8$^{-/-}$ (n = 16), TRPV1$^{+/-}$ (n = 8), and TRPV1$^{-/-}$ (n = 14) male mice and equal numbers of female mice, never exposed to mating after weaning and, therefore, sexually naive, were observed in mating assays. An estrous female

was added to the male's home cage and the latency and frequency of mounting, intromission, and ejaculation were recorded over 2 hours. All animals exhibited mounting and intromission during this period. Most of the sexually inexperienced males in TRPM8$^{-/-}$mated to ejaculation.

Mating assays were performed between 19:00 and 21:00. Each male was housed individually in a plexi-glass cage (12" × 12" × 12"; $l \times w \times h$) at 17:00 hours. All mice were given food and water ad libitum. For mating behavior experiments, a sexually receptive female (TRPM8$^{+/+}$, TRPM8$^{+/-}$, TRPM8$^{-/-}$, TRPV1$^{+/-}$, or TRPV1$^{-/-}$) was transferred into the cage where a respective male strain was housed. They were housed together for 2 hours. All behaviors were videotaped, and an experienced observer, blinded to the type of mouse strains used for mating behavior studies, quantified the following parameters during the 2-hour test period. The following parameters were analyzed and quantified: 1) the number of events of mounting a female with or without intromission; 2) the latency between mounting; 3) the frequency and duration of males mounting a female or male; and 4) the rates of ejaculation.

2.1.3 | Aggression Assay

We used a resident-intruder paradigm to test for aggressive behavior of mice (10-12 weeks old, male). Each mouse was individually housed in a plexi-glass cage that was not cleaned for 3 days prior to the test. Interactions between the resident mice with an unfamiliar intruder mouse were video-recorded for a period of 2 hours. The aggressive behavior between the two animals (latency to a first attack, the total number of bite attacks, and the duration of attacks) was then scored.

2.1.4 | Mating assay and time to first mount

Male mice were tested before and after mating experience for 10 days. Male mice used for mating were tested for aggressive behaviors as well. The testing period lasted 12 hours The test started when each mouse strain male and an estrous female were placed in the cage of the test. All parameters of mating and aggressive behavior were scored. Also, the number of times the male mouse mounted the male was also recorded in separate experiments. We also recorded the time to first mounting between each pair of male and estrous female of individual mouse strains.

2.1.5 | Sniffing behavior

Age-matched male and female TRPM8$^{+/+}$, TRPM8$^{+/-}$, and TRPM8$^{-/-}$ mice were used for the study. The mice were allowed to sniff either a cotton swab soaked with urine (test) or an unsoaked (unsoiled control) cotton swab during the assay in a closed cage. The number of times the mouse sniffed the soaked/unsoaked cotton swab for a total period of 5 minutes was counted and expressed as sniffs per minute.

Condition 1: Male and estrous female TRPM8$^{+/+}$, TRPM8$^{+/-}$, and TRPM8$^{-/-}$ mice were allowed to sniff an unsoiled cotton swab or a cotton swab soaked with urine (200 μL) that was obtained from estrous female and male mice, respectively, of the same strain.

Condition 2: Male and estrous female TRPM8$^{+/+}$, TRPM8$^{+/-}$, and TRPM8$^{-/-}$ mice were allowed to sniff an unsoiled cotton swab or a cotton swab soaked with urine (200 μL) that was obtained from the compared strain of estrous female and male mice, respectively.

2.1.6 | Serum testosterone and estradiol concentration determination

Testosterone and 17β-estradiol concentrations were determined using 100 μL of blood obtained by retro-orbital bleeding into heparin solution and processed using ELISA kit for testosterone (ADI-900-065) and 17β-estradiol (ADI-900-174), following the procedure described by the manufacturer (ENZO Life Sciences, USA). The samples were then taken for the ELISA assay, where concentrations of testosterone or 17β-estradiol were measured at 405 nm on a plate-reader (Glomax, Promega, USA).

2.2 | Testing of acute testosterone applications on brain slices

2.2.1 | Mouse brain slices experiments

For investigations of exogenous testosterone application on brain slices 3 to 4-month-old mice (n = 13 total) of both sexes were used, including seven WT (four males, three females) and six TRPM8$^{-/-}$ (three males, three females) mice. The experimenter was blinded to the identity of the mouse. All procedures were approved by the Institutional Animal Care and Use Committee (IACUC, protocol #16164) at University of Illinois Urbana-Champaign. Animals were housed in animal care facilities at the Beckman Institute for Advanced Science and Technology, approved by the American Association for Accreditation of Laboratory Animal Care (AAALAC).

2.2.2 | Brain slicing

Mice were initially anesthetized with ketamine (100 mg/kg) and xylazine (3 mg/kg) intraperitoneally and perfused with

chilled (4°C) sucrose-based slicing solution (234 mM sucrose, 11 mM glucose, 26 mM $NaHCO_3$, 2.5 mM KCl, 1.25 mM NaH_2PO_4, 10 mM $MgCl_2$, 0.5 mM $CaCl_2$) containing 1 mM kynurenic acid to preserve neuronal viability.[14] Four 300 μm-thick coronal brain slices containing centromedial amygdala (corresponding to coronal slices #66-71 of the Allen Mouse Brain Atlas[15]) per animal were obtained and transferred into a covered incubation chamber with incubation solution (10 mM glucose, 126 mM NaCl, 3 mM $MgCl_2$, 1 mM $CaCl_2$, 2.5 mM KCl, 1.25 mM NaH_2PO_4, 26 mM $NaHCO_3$). About 5 μL of 1 mM Fluo-4 AM solution (50 μg of Fluo-4 AM dissolved in 48 μL of DMSO and 2 μL of Pluronic F-127) was pipetted onto each brain slice,[16] resulting in a final concentration of 13.3 μM of Fluo-4 AM in the incubation chamber, wherein slices were incubated at 37°C for 30 minutes while the solution was bubbled with 95% oxygen/5% carbon dioxide. Slices were then transferred to a fresh incubation solution without Fluo-4 AM and Pluronic F-127, where they remained for 20 minutes at room temperature while the solution was being bubbled with 95% oxygen/5% carbon dioxide. After incubation, slices were transferred to a perfusion chamber of a Nikon Eclipse E600FN microscope and perfused with artificial cerebrospinal fluid (aCSF) (10 mM glucose, 126 mM NaCl, 2 mM $MgCl_2$, 2 mM $CaCl_2$, 2.5 mM KCl, 1.25 mM NaH_2PO_4, 26 mM $NaHCO_3$) bubbled with 95% oxygen/5% carbon dioxide. At least 10 minutes of equilibration time was given before imaging.

2.2.3 | Fluorescence imaging and image acquisition

Images of centromedial amygdala were collected with a QImaging OptiMOS sCMOS camera with 4X4 binning, 100 ms exposure (100.2 ms average acquisition period) and at 20x magnification (Nikon Fluor 20X/0.50W water immersion objective) using MicroManager software (https://micro-manager.org/). During image acquisition, 450-495 nm excitation light was delivered to the tissue *via* a Prior *Lumen 200* Fluorescence Illumination System (100W) through the objective and emitted fluorescence was collected at a range of 515-555 nm through the objective. For each slice, 200 frames were collected prior to the application of vehicle or testosterone solution, which are referred to as baseline frames. Then 2000 frames were collected during the treatment with the vehicle or testosterone solution, which are referred to as vehicle or testosterone frames, respectively.

2.2.4 | Vehicle and testosterone solution application

For testosterone, 1 mL of 0.1 μM testosterone solution bubbled with 95% oxygen/5% carbon dioxide was placed into a syringe and applied to the brain slice in the perfusion chamber *via* a Kd Scientific single syringe infusion pump. About 1 mL of the testosterone solution was injected over the course of 2 minutes and 10 seconds, bringing the final concentration of testosterone in the perfusion chamber to 10 nM. This concentration was selected after a set of pilot experiments that enabled most optimal signal-to-noise ratio, and corresponds to concentrations used in other in vitro preparations.[17-20] Vehicle controls consisted of ethanol dissolved in aCSF at the same concentration as the testosterone solution (final concentration of ethanol = 0.0001%). At 1 minute and 40 seconds of the testosterone solution application, which is approximately the time taken for more than a third of the solution to reach the perfusion chamber, imaging was initiated and continued for 200 seconds, acquiring 2000 frames. For vehicle application, all of the above steps were repeated, but with 1 mL of vehicle in aCSF bubbled with 95% oxygen/5% carbon dioxide.

2.2.5 | Image processing and statistical analysis

For the sequence of frames collected for each imaged brain slice, regions of interest (ROIs) were manually drawn around visible neurons with ImageJ software. For all 2200 frames of the slice, the average pixel intensity was calculated for each ROI. For each ROI, the sequence of these average pixel intensities for the 200 baseline frames and the 2000 vehicle/testosterone application frames were detrended using the detrend function of MATLAB as well as the Teodorescu method for nonlinear detrending.[21] The standard deviation was computed in 200 frame blocks over the course of 2200 frames obtained for each cell. The difference of the standard deviation at 60 seconds post-infusion to baseline was considered the magnitude of the response for that cell. 60 seconds was used because this time point was found to display the maximal response to the drug application. This magnitude was normalized by subtracting the average response of each cell in that slice to account for slice-to-slice variability in calcium indicator uptake. For each animal, a classification threshold was calculated for the collection of the normalized response differences across all of the animal's cells. This classification threshold was set to be 2.5 times the standard deviation of those normalized response magnitudes for the animal's cells. For each animal, any cells whose normalized response magnitude was equal to or greater than the animal's classification threshold were classified as active cells, and all other cells were classified as non-active cells.

The total number of active cells and total number of non-active cells were counted for five categories: WT males, WT females, $TRPM8^{-/-}$ males, and $TRPM8^{-/-}$ females for the testosterone application, and a WT male for the vehicle

application. For each category, the percentage of active cells was calculated. Between WT and TRPM8$^{-/-}$ mice of the same sex, for the testosterone application, a chi-square test was performed to determine if the differences in percentage of active cells were significant.

All calculations were performed using MATLAB R2016 and Excel 2016.

2.3 | In situ hybridization

The in situ hybridization (ISH) Buffer and Controls Kit and double DIG labelled /5DigN/ TGTAGAAGTAAGCGAAGACGAT/3Dig_N/ - custom LNA TRPM8 mRNA hybridization probe were purchased from Exiqon (Woburn, MA). The detailed procedure for ISH was done following the supplied protocol. In brief, paraffin-embedded tissue sections were subjected to deparaffinization and following steps were performed: proteinase-K treatment at 37°C, pre-hybridization at 55°C for 15 minutes, hybridization with DIG-labeled LNA TRPM8 mRNA probe (50 nM), at 55°C for 60 minutes, stringent washes with SSC buffers at 55°C for over a total of 33 minutes followed by DIG blocking reagent (15 min at RT), alkaline phosphatase-conjugated anti-DIG at 1:1000 dilution (60 min at RT), alkaline phosphatase-substrate; enzymatic development (120 min at RT), and nuclear fast red counterstain (5 min). The slides were mounted, air-dried, and the images were captured with a light microscope (Olympus IX71, Minneapolis, MN) at a 10, 20, or 40X magnification.

2.4 | Immunohistochemistry

Brain slices were processed for immunohistochemical (IHC) analysis according to the standard protocol.[22] The brain tissue sections were deparaffinized in xylene and rehydrated in graded ethanol solutions. Antigen retrieval was carried out with 10 mM EDTA-Tris buffer (pH 9.0) at boiling temperature for 20 minutes, followed by 20 minutes cooling incubation in the same buffer, and permeabilization in 0.2% Triton-X-100. Alternatively, frozen brain slices were processed directly to the blocking step. The sections were blocked using 10% bovine-serum albumin (BSA) in phosphate-buffered saline (PBS) and then, incubated with primary antibodies overnight at room temperature. We used anti-TRPM8 antibodies (Phoenix Pharmaceuticals, Burlingame, CA), neuronal marker NeuN or anti-FOX3 antibody (Thermo Fisher Scientific, Waltham, MA), pyramidal neurons marker CaMKIIα antibody (Invitrogen, obtained from Thermo Fisher), testosterone 3-(O-carboxymethyl)-oxime-BSA-fluorescein isothiocyanate conjugate (testosterone-BSA-FITC) (Sigma Aldrich, Burlington, MA), where the OB slices were treated with 1 nM Testosterone-BSA-FITC for 2 hours. For dopaminergic (DA) neurons detection tyrosine hydroxylase (TH) was used as a DA marker, readily recognized by anti-TH antibody (Millipore, Kankakee, IL). As a marker of neuronal activity cFos protein was detected using anti-cFos antibody (Thermo Fisher Scientific).

To optimize the antibody labeling sensitivity, all primary antibody treatments were done in Da Vinci Green buffer (Biocare Medical, LLC, Pacheco, CA). The slices were washed with PBS and incubated with fluorescent-labeled, species-specific secondary antibodies (Alexa Fluor) at 1:1000 dilution for 2 hours at room temperature. Before mounting, the slides were washed with PBS and incubated for 5 minutes with 1:100 dilution of 4'-6-diamidino-2-phenylindole (*DAPI*) for nuclear staining and analyzed using Olympus BX61 confocal microscope (Minneapolis, MN) (20X, 40X, or 60X objectives).

2.5 | Planar lipid bilayer experiments

2.5.1 | Preparation of the TRPM8 protein from HEK cells

HEK-293 cells stably expressing TRPM8 tagged with *myc* on the N-terminus were grown to 70%-80% confluence, washed, and collected with PBS, as previously described.[23] Cells were harvested and resuspended in NaCl-based (NCB) buffer, containing 500 mM NaCl, 50 mM NaH_2PO_4, 20 mM HEPES, 10% Glycerol, pH 7.5, with addition of 1 mM of protease-inhibitor PMSF, 5 mM β-Mercaptoethanol. The cells were lysed by freeze-thawing method and centrifuged at low speed to remove cell-debris and DNA. The supernatant was further centrifuged at 40 000 *g* for 2.5 hours, and the pellet was resuspended in NCB buffer with addition of a protease inhibitor cocktail (Roche, Indianapolis, IN), 0.1% Nonidet P40 (Roche) and 0.5% dodecyl-maltoside (DDM) (CalBiochem, EMD). The suspension was incubated overnight at 4°C on a shaker with gentle agitation and then, centrifuged for 1 hour at 40 000 *g*. Further, the TRPM8 protein was purified by immunoprecipitation with anti-Myc-IgG conjugated to A/G protein magnetic beads (Pierce, Thermo Fisher Scientific), following the procedure provided by the manufacturer. All steps of purification were performed at 4°C. For the planar lipid bilayers experiments, the protein was eluted with myc-peptide (150 μg/ml).

2.5.2 | Mass spectrometry analysis

After the immunoprecipitation and purification TRPM8 protein was separated by SDS-PAGE and stained with Coomassie blue. The resulted bands were excised from the

gel and digested with trypsin for mass spectrometry analysis according to Mann et al protocol,[24] with some modifications. Briefly, the gel bands were reduced with 0.5 M dithiothreitol and alkylated with 0.7 M iodoacetamide. Gel bands were digested with trypsin (Promega, Madison, WI) for 12 hours at 37°C. Peptides were extracted from the gel bands with 100 µL of a 50% acetonitrile 5% formic acid solution. The extract was dried by vacuum centrifugation (SPD SpeedVac Thermo Electron Corp. Waltham, MA); the tryptic peptides were resuspended in 20 µL of a 3% acetonitrile, 0.5% formic acid solution.

Liquid chromatography-tandem mass spectrometry (LC-MS/MS) was performed using a nano flow liquid chromatography system (Ultimate3000, Thermo Scientific) interfaced to a hybrid ion trap-orbitrap high-resolution tandem mass spectrometer (VelosPro, Thermo Scientific) operated in data-dependent acquisition (DDA) mode. Briefly, one microliter of each sample was injected onto a capillary column (4 µm Jupiter C18 manually packed on a 30 cm × 75 µm ID PicoFrit Column, New Objective) at a flow rate of 300 nL/min. Samples electro-sprayed at 1.2 kV using a dynamic nanospray ionization source. Chromatographic separation was carried out using 90-minute linear gradients (Mobile Phase A: 0.1% formic acid in MS-grade water, mobile phase B: 0.1% formic acid in MS-grade acetonitrile) from 3% B to 35% B over 60 minutes, then increasing to 95% B over 5 minutes. MS/MS spectra were acquired using both collision-induced dissociation (CID) and higher-energy collisional dissociation (HCD) for the top 15 peaks in the survey 30000-resolution MS scan. The.raw files were acquired (Xcalibur, Thermo Fisher) and exported to Proteome Discoverer 2.0 (Thermo Fisher) software for peptide and protein identification using SequestHT search algorithm (Full trypsin digestion with two maximum missed cleavages, 10 ppm precursor mass tolerance and 0.8 Da fragment F tolerance). Database searching was done using the UniprotKB database.

2.5.3 | Planar lipid bilayer measurements

Planar lipid bilayers measurements were performed as previously described.[23,25,26] Briefly, lipid bilayers were formed from a solution of synthetic 1-palmitoyl-2-oleoyl-glycero-3-phosphocoline (POPC) and 1-palmitoyl-2-oleoyl-glycero-3-phosphoethanolaminein (POPE, Avanti Polar Lipids, Birmingham, AL) in ratio 3:1 in n-decane (Aldrich). The solution was used to paint a bilayer in an aperture of ~150 µm diameter in a Delrin cup (Warner Instruments, Hamden, CT) between symmetric aqueous bathing solutions of 150 mM KCl, 0.02 mM $MgCl_2$, 1 µM $CaCl_2$, 20 mM Hepes, pH 7.2, at 22°C. All salts were ultrapure (>99%) (Sigma-Aldrich). Bilayer capacitances were in the range of 50-75 pF. After the bilayers were formed, the TRPM8 protein from micellar solution (20 ng/mL) was added by painting. Unitary currents were recorded with an integrating patch clamp amplifier (Axopatch 200B, Axon Instruments). The *trans* solution (voltage command side) was connected to the CV 201A head stage input, and the *cis* solution was held at virtual ground *via* a pair of matched Ag-AgCl electrodes. Currents through the voltage-clamped bilayers (background conductance < 1 pS) were filtered at the amplifier output (low pass, −3 dB at 10 kHz, 8-pole Bessel response). Data were secondarily filtered at 100 Hz through an 8-pole Bessel filter (950 TAF, Frequency Devices) and digitized at 1 kHz using an analog-to-digital converter (Digidata 1322A, Axon Instruments), controlled by pClamp10.3 software (Axon Instruments). Single-channel conductance events, all points' histograms, open probability, and other parameters were identified and analyzed using the Clampfit10.3 software (Axon Instruments).

2.6 | Statistical analysis

Statistical analyses were performed using Origin 9.0 software (Microcal Software Inc, Northampton, MA, USA). Statistical significance was calculated using one-way ANOVA followed by Fisher's LSD test and data were expressed as mean ± SEM $P < .05$ was considered to be significant. In all figures, statistical significance is labeled the following way: $*P < .05$, $**P < .01$, $***P < .001$, and $****P < .0001$.

3 | RESULTS

3.1 | TRPM8 regulates sexual satiety and consummatory aspects of testosterone-driven sexual behaviors

Testosterone is required for systemic activation of sexual behavior in the majority of vertebrates.[27,28] As an ionotropic testosterone receptor of the orphan rapid signaling mechanism,[7,8] TRPM8 may play a role in testosterone-dependent behaviors. To test this hypothesis, we performed a set of behavioral experiments using TRPM8 knockout (KO, or $TRPM8^{-/-}$) mice, with the WT or $TRPM8^{+/+}$, and $TRPM8^{+/-}$ strains as controls. Since TRPM8 is a critical temperature receptor,[29,30] as an alternative control we also used the mutant mice deficient in another thermosensitive TRP channel from the Vanilloid subfamily 1 (TRPV1), implying heterozygous ($TRPV1^{+/-}$) and homozygous ($TRPV1^{-/-}$) strains as relative $TRPM8^{+/+}$ controls. Initially, our design included assessing the mating behavior of $TRPM8^{-/-}$ males toward WT females. However, in the experimental settings with a WT female and a $TRPM8^{-/-}$ male, the low receptive response of the female to the sexual vigor of $TRPM8^{-/-}$ resulted in a

strong aggression of the TRPM8$^{-/-}$ male toward the female, causing a severe injury of the latter. This complication resulted in reassessing the mating within the same genotypes.

Strikingly, we observed that compared to the controls, TRPM8$^{-/-}$ male mice displayed a markedly increased frequency in mounting TRPM8$^{-/-}$ females (Figure 1A, Supporting Figure S1A). The durations of mounting were slightly reduced in TRPM8$^{-/-}$ strain (Figure 1B, Supporting Figure S1B). A further difference was noticed in the intromission time, which was markedly shorter compared to controls (Figure 1C, Supporting Figure S1C), while ejaculations did not change significantly across all the tested stains (Figure 1D, Supporting Figure S1D).

The time latency prior to the initiation of copulation is a measure of sexual motivation. It is sensitive to the levels of both testosterone and estrogen and is relevant to dopamine release in the medial preoptic area.[31] Assessing the latency to first mounting, we found TRPM8$^{-/-}$ mice to exhibit stronger sexual motivation than control animals as indicated by a significantly shortened latency (Figure 1E, Supporting Figure S1E). The pattern of mountings was also altered, showing a reduction in the percentage of short-duration (<8 s) mounts and a corresponding increase in that of long-duration (>8 s) mounts in TRPM8$^{-/-}$ mice (Figure 1F, Supporting Figure S1F). It is also important to note that ejaculations (Figure 1D, Supporting Figure S1D) were only

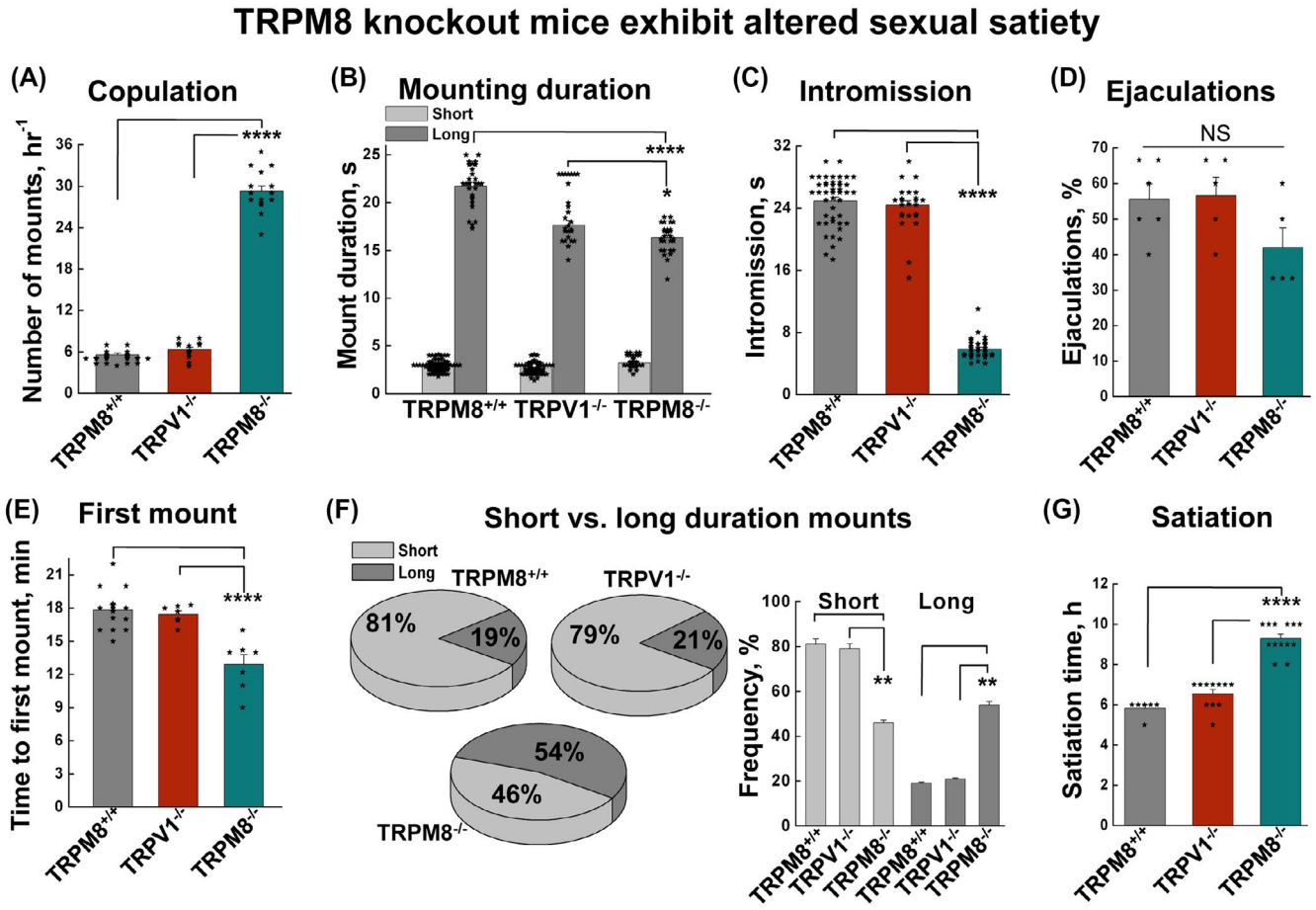

FIGURE 1 TRPM8 knockout mice demonstrate altered sexual behaviors. Mounting behavior was analyzed using mice of the same strain to compare the performances among the TRPM8$^{+/+}$, TRPV1$^{-/-}$, and TRPM8$^{-/-}$. A, TRPM8$^{-/-}$ male mice showed increased number of mountings ($P = 4.86 \times 10^{-27}$ for TRPM8$^{+/+}$ vs TRPM8$^{-/-}$, and $P = 7.47 \times 10^{-21}$ for TRPV1$^{-/-}$ vs TRPM8$^{-/-}$). B, mounting durations were decreased in TRPM8$^{-/-}$ ($P = 2.5 \times 10^{-15}$ for TRPM8$^{+/+}$ vs TRPM8$^{-/-}$, and $P = .016$ for TRPV1$^{-/-}$ vs TRPM8$^{-/-}$). C, TRPM8$^{-/-}$ mice exhibited reduced intromission duration ($P = 3.15 \times 10^{-44}$ for TRPM8$^{+/+}$ vs TRPM8$^{-/-}$, and $P = 3.09 \times 10^{-40}$ for TRPV1$^{-/-}$ vs TRPM8$^{-/-}$). D, ejaculation rates were not significantly (NS) different. E, the time to first mount was reduced in TRPM8$^{-/-}$ mice ($P = 1.19 \times 10^{-4}$ for TRPM8$^{+/+}$ vs TRPM8$^{-/-}$, and $P = 4.29 \times 10^{-4}$ for TRPV1$^{-/-}$ vs TRPM8$^{-/-}$). F, TRPM8$^{-/-}$ mice exhibited more frequent long-duration mounting (>8 s) than short duration mounting (<4 s) (for long durations $P = .0018$ for TRPM8$^{+/+}$ vs TRPM8$^{-/-}$, and $P = .0034$ for TRPV1$^{-/-}$ vs TRPM8$^{-/-}$, and for short durations $P = .0032$ for TRPM8$^{+/+}$ vs TRPM8$^{-/-}$, and $P = .0023$ for TRPV1$^{-/-}$ vs TRPM8$^{-/-}$). G, mating satiety time was estimated as the duration of mounting activities before a complete inhibition within the active period of the circadian cycle, which was significantly longer for TRPM8$^{-/-}$ ($P = 7.3 \times 10^{-9}$ for TRPM8$^{+/+}$ vs TRPM8$^{-/-}$, and $P = 4.22 \times 10^{-9}$ for TRPV1$^{-/-}$ vs TRPM8$^{-/-}$). Data are the mean of a minimum of eight experiments, each performed using a sexually inexperienced male and female pair. Error bars represent ± s.e.m. Statistical significance was evaluated using one-way ANOVA test

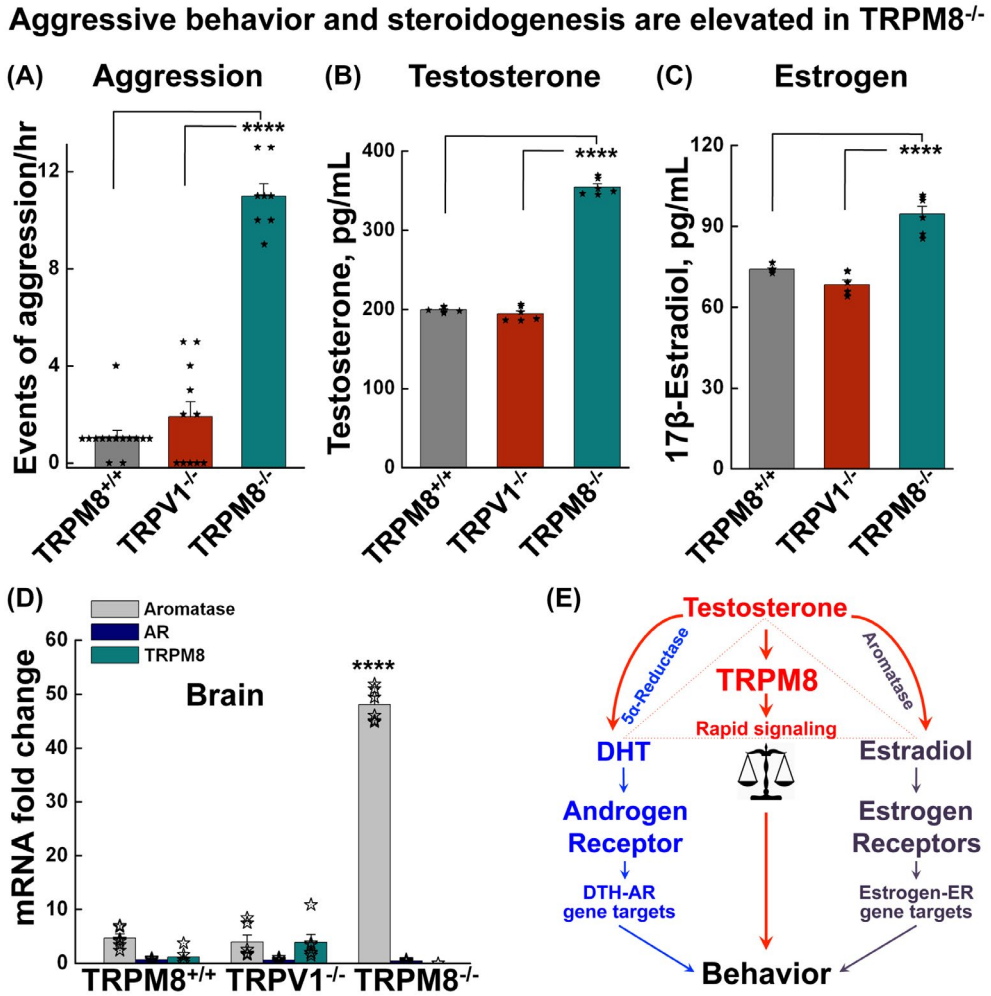

FIGURE 2 TRPM8$^{-/-}$ mice show increased aggressive behavior and elevated serum testosterone levels. A, the aggression of male animals was assessed as number of attacks for TRPM8$^{+/+}$, TRPV1$^{-/-}$, and TRPM8$^{-/-}$ mice as mean ± s.e.m. of at least 12 experiments (one conspecific pair in each experiment). $P = .208$ for TRPM8$^{+/+}$ vs TRPV1$^{-/-}$; $P = 6.195 \times 10^{-14}$ for TRPM8$^{+/+}$ vs TRPM8$^{-/-}$; and $P = 5.747 \times 10^{-9}$ for TRPV1$^{-/-}$ vs TRPM8$^{-/-}$. B, serum testosterone concentrations determined by ELISA. Data are mean ± s.e.m., for males of the TRPM8$^{+/+}$ (n = 6), TRPV1$^{-/-}$ (n = 6) and TRPM8$^{-/-}$ (n = 6) mice. $P = .315$ for TRPM8$^{+/+}$ vs TRPV1$^{-/-}$; $P = 3.699 \times 10^{-5}$ for TRPM8$^{+/+}$ vs TRPM8$^{-/-}$; and $P = 6.586 \times 10^{-5}$ for TRPV1$^{-/-}$ vs TRPM8$^{-/-}$. C, serum 17β-estradiol concentrations determined by ELISA. Data are mean ± s.e.m., for males of the TRPM8$^{+/+}$ (n = 6), TRPV1$^{-/-}$ (n = 6), and TRPM8$^{-/-}$ (n = 6) mice. $P = .262$ for TRPM8$^{+/+}$ vs TRPV1$^{-/-}$; $P = 1.15 \times 10^{-6}$ for TRPM8$^{+/+}$ vs TRPM8$^{-/-}$; and $P = 4.5 \times 10^{-5}$ for TRPV1$^{-/-}$ vs TRPM8$^{-/-}$. D, mRNA levels determined by quantitative RT-PCR for aromatase, androgen receptor, and TRPM8 in brains of the TRPM8$^{+/+}$, TRPV1$^{-/-}$, and TRPM8$^{-/-}$ male mice (n = 4 each). All probes were normalized to glyceraldehyde 3-phosphate dehydrogenase (GAPDH). $P = 2.96 \times 10^{-7}$ for TRPM8$^{+/+}$ vs TRPM8$^{-/-}$, and $P = 2.25 \times 10^{-8}$ for TRPV1$^{-/-}$ vs TRPM8$^{-/-}$ of aromatase. Statistical significance was evaluated using one-way ANOVA test. E, schematic illustration of behavioral regulation by testosterone and its metabolic products, dihydrotestosterone (DHT) and estradiol. Testosterone activates rapid signaling through TRPM8 and its products induce genomic pathways through nuclear receptors, with DHT acting at androgen receptor (AR) and estradiol at estrogen receptors (ERs). Testosterone is converted to DHT by 5α-reductase and estradiol by aromatase

observed after the long-duration mounts but not the short ones.

To assess the sexual satiation state, we estimated how long it took for TRPM8$^{-/-}$ mice to stop their mating activities. In general, sexual satiation is defined as lasting sexual inhibition after repeated copulations.[32] We found that during the active period of the circadian cycle, the control mice reached their satiation at around 4-6 hours, while it took TRPM8$^{-/-}$ mice almost 10 hours to stop their mounting behavior (Figure 1G). Together, these results further suggest that TRPM8$^{-/-}$ animals exhibit delayed sexual satiety.

3.2 | TRPM8 controls male territorial behavior and aggression

Next, we assessed the role of TRPM8 in territorial behaviors and aggression, which are typical male behavioral attributes

of testosterone. Previously, testosterone-induced aggression had been characterized in male mice with genetic ablation of genomic steroid receptors, such as androgen and estrogen receptors. While male mice lacking androgen receptor (AR) in the brain exhibited reduced aggression and spent less time fighting with cage mates without a reduction in the number of initiated attacks,[27] those lacking estrogen receptor α (ERα-KO) displayed virtually no aggressive behavior, even with testosterone administration, a treatment that induces aggression in the WT mice.[33] In line with these reports, male mice null for aromatase, the enzyme that converts testosterone to estrogen, also displayed profound deficits in aggression, further implying a critical role of estrogen in male-typical aggression.[34-36] However, contrary to the above findings about genomic steroid receptors, TRPM8$^{-/-}$ males exhibited more aggression toward their conspecifics, as shown by the approximately 10-fold increase in the number of attacks per hr than the control animals (Figure 2A). As another control, TRPV1$^{-/-}$ males did not show more aggression than WT males. These results suggest that the lack of TRPM8 provokes an enhanced aggressive phenotype in males. This behavior could arise from a previously unrecognized negative action of TRPM8 downstream signaling on aggression or, given the established role of genomic receptors in male aggression and the ability of TRPM8 to modulate systemic testosterone levels, from the altered steroid milieu due to TRPM8 deficiency.

To determine whether the increased aggressive behavior of TRPM8$^{-/-}$ mice was, in fact, due to the altered steroid levels, we measured serum testosterone concentrations in these animals. Indeed, TRPM8$^{-/-}$ male mice exhibited markedly elevated concentrations of serum testosterone compared to the age-matched TRPM8$^{+/+}$ and TRPV1$^{-/-}$ strains (Figure 2B). These results further suggest that the absence of TRPM8 function modulates a feedback mechanism that results in increased testosterone production, through which TRPM8 essentially controls circulating testosterone levels.

Considering the role of ERα in male-aggressive behaviors[33] and the fact that testosterone is a direct precursor of 17β-estradiol, a specific type of estrogen, we also measured the concentration of this metabolite. As anticipated, the serum concentration of 17β-estradiol was significantly upregulated in TRPM8$^{-/-}$ males (Figure 2C). While these results indicate that steroid concentrations are elevated in the circulation and peripheral tissues, in order to determine the capacity of TRPM8$^{-/-}$ to produce 17β-estradiol in the brain, we measured the messenger RNA of aromatase—the enzyme that converts testosterone to estrogen. Using quantitative real-time PCR, we showed that the mRNA level of aromatase was markedly upregulated in the brain of TRPM8$^{-/-}$ males (Figure 2D), further supporting the idea that the enhanced aggressive phenotype of these mice could arise, at least in part, from an increase in steroidogenesis (Figure 2E).

Notably, the levels of both testosterone and 17β-estradiol were also upregulated in TRPM8$^{-/-}$ female mice (Supporting Figure S2). Together, these results suggest that TRPM8 systemically regulates steroidogenesis in both sexes.

3.3 | TRPM8 sensitivity to testosterone exceeds that to estradiol and progesterone

Given that along with testosterone TRPM8 also regulates levels of estrogen (Figure 2B,C, and Supporting Figure S2), we questioned whether the channel is also functionally implicated in the signaling of the prevalent female hormones. Therefore, we tested the sensitivity of TRPM8 to these steroids, including progesterone and 17β-estradiol.

To unambiguously assess the effects of steroid hormones on TRPM8 channel function, we evaluated TRPM8 activity in a steroid-free reconstituted system. TRPM8 protein was purified and incorporated in the bilayers as described previously.[8,23,25,26,37] The purity of TRPM8 protein in the samples was confirmed by liquid chromatography-mass spectrometric (LC-MS/MS) analysis (Supporting Figure S3). Importantly, purified TRPM8 protein samples did not contain any other detectable levels of contaminant ion channels, or androgen-related proteins. The complete list of proteins co-precipitated with TRPM8 can be found in our previous work.[8]

To establish the precise mechanism of TRPM8-steroid interactions at each side of the leaflet, we first examined the effect of the membrane-impermeable analog—testosterone covalently conjugated to BSA (BSA-testosterone). BSA-testosterone was shown to elicit rapid Ca^{2+} influx in the prostate cells.[8,38] This effect of testosterone suggested that one of the binding sites to the channel is located at its extracellular domain.[8] Herein, we tested BSA-testosterone effect on TRPM8 reconstituted in lipid bilayers and found that this analog activated TRPM8 from the external side only (Supporting Figures S4 and S5). Similar to the permeable testosterone, BSA-testosterone-induced TRPM8 activity at picomolar solution concentrations, but induced openings of a distinct gating mode and small conductance state (Supporting Figure S4). The mean slope conductance of BSA-testosterone-induced TRPM8 was ~7 pS, in comparison to 37 pS of testosterone-induced conductance (Supporting Figure S4). Importantly, addition of the membrane-permeable testosterone to the external side of TRPM8 exerted similar openings of ~7 pS magnitude, and a consequent application of the steroid to the internal side further increased its conductance to ~37 pS (Supporting Figure S5). These results suggest that the particular steroid binding pockets on TRPM8 exert discrete conformational changes by affecting both—the permeation path and the gating of the channel.

Next, we assessed the selectivity of TRPM8 to different steroids. We found that in contrast to testosterone that activated TRPM8 with an EC_{50} of 22.4 ± 0.47 pM, and dihydrotestosterone (DHT), a derivative with ~1000 fold less potency (EC_{50} of 23.5 ± 0.98 nM), both progesterone and 17β-estradiol induced the channel activity only at high concentrations (Figure 3A,B), exhibiting EC_{50} values of 0.49 ± 0.05 μM and 1.2 ± 0.12 μM, respectively (Figure 3C). Notably, both 17β-estradiol and progesterone added to both sides of the bilayers-induced TRPM8 opening only into a small conductance state, similar to that of membrane-impermeable BSA-testosterone (Figure 3A,B, and Supporting Figures S4 and S5). Importantly, when activated with a membrane-permeable testosterone, or BSA-testosterone, progesterone, and 17β-estradiol, the TRPM8 channel demonstrated not only a distinct conductance state but also an altered gating mode, further suggesting the presence of at least two interacting sites for the steroids. The inner binding pocket can be accessed by a permeable testosterone, but not BSA-testosterone, while the external binding site is accessible to all other steroid hormones listed above. Together, these results support the premise that TRPM8 is primarily a testosterone receptor. Other steroids induce channel openings at almost five-order of magnitude higher concentrations. Therefore, testosterone is not only a highly potent but also a highly specific agonist of the TRPM8 channel.

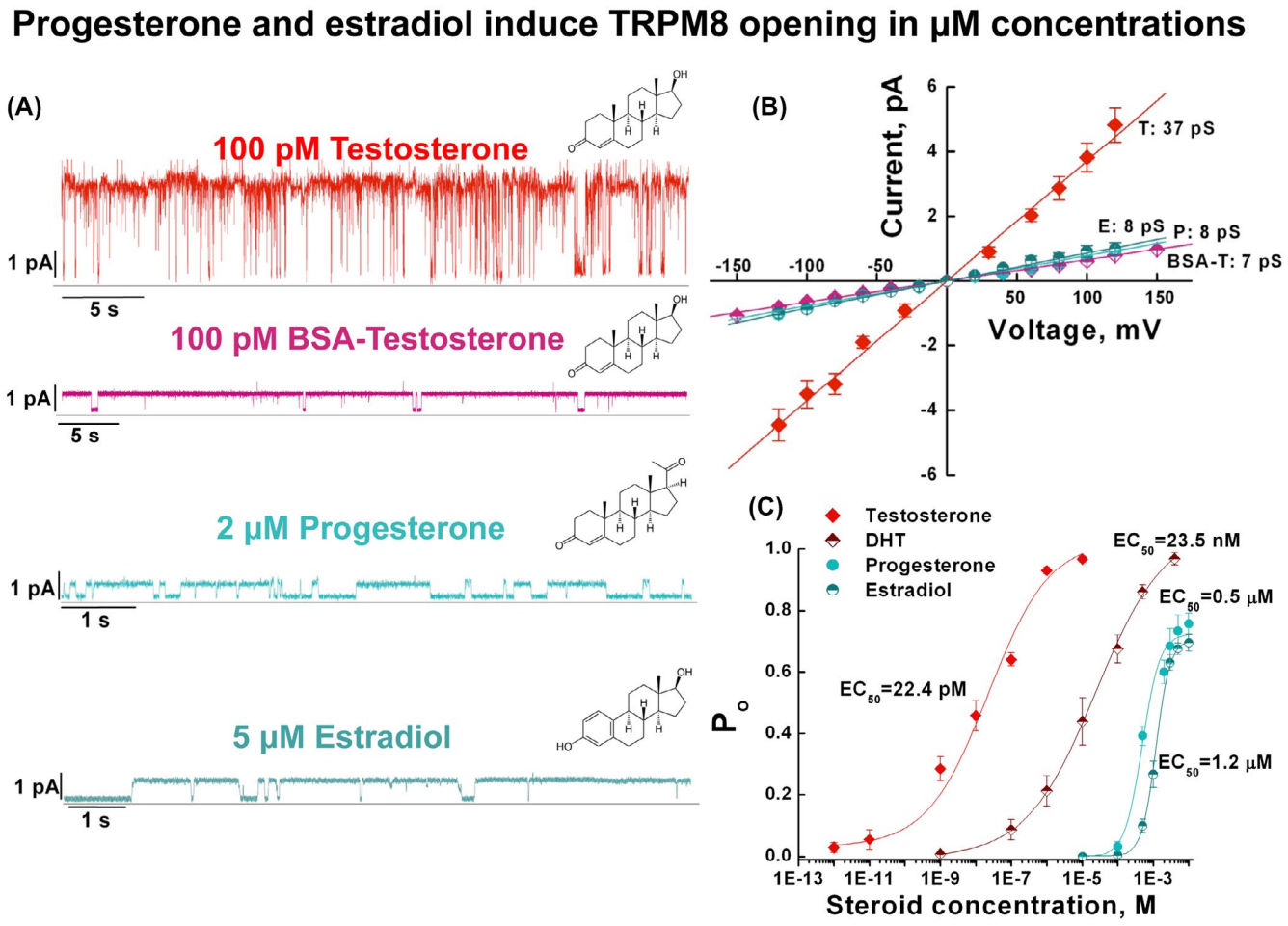

FIGURE 3 TRPM8 is primarily activated by testosterone. TRPM8 channel activity was assessed in planar lipid bilayers in the presence of varying concentrations of steroid hormones: testosterone (or membrane impermeable BSA-testosterone), dihydrotestosterone (DHT), progesterone, and estradiol. All stock solutions of the membrane-permeable steroids were prepared in ethanol, which upon application were diluted 1/1000, reaching a final concentration of ethanol 0.1%. BSA-testosterone stock solution was prepared in the phosphate buffer, pH 7.5. A, representative single channel currents at 100 mV of TRPM8 activated in the presence of indicated steroids and 2.5 μM DiC_8 PIP_2. Note BSA-testosterone-, progesterone-, and estradiol-induced TRPM8 openings only into the small conductance state. B, current-voltage (I-V) relationship for TRPM8 currents induced by testosterone (T), 17β-estradiol (E), progesterone (P), and BSA-testosterone (BSA-T). C, concentration response curves of TRPM8 activation by testosterone, DHT, progesterone, and estradiol obtained in the presence of 2.5 μM DiC_8 PIP_2 at 60 mV, number of events (channel gating) analyzed for progesterone = 247,520 and for estradiol = 281,483. Data points represent mean ± s.e.m. of n = 51 experiments and were fitted by linear regression (B) or Hill equation (C), which yielded single channel conductance and EC_{50} values, respectively, as shown

3.4 | TRPM8$^{-/-}$ mice exhibit altered sexual preferences

The tuned balance of steroid hormones regulates mating choice behaviors.[39,40] To assess the role of TRPM8 in this behavioral repertoire, we next analyzed the mating behaviors of TRPM8$^{-/-}$ mice in a mating choice assay. Curiously, TRPM8$^{-/-}$ male mice displayed increased mating frequency indiscriminate of sexes, with markedly increased attempts to mount both females and males (Figure 4A,B).

Notably, although sexual interactions between same-sex partners (male mounting over male, or female mounting over female) can be observed in animals in captivity, such behaviors are expressed mostly when the opposite sex is unavailable.[41] However, the TRPM8$^{-/-}$ male mice made more attempts to mount each other than the estrous female present in the same cage (Figure 4C). This atypical mounting behavior of TRPM8$^{-/-}$ male mice suggests either an altered sexual preference or an impaired ability to distinguish among sexes, further highlighting the role of TRPM8 in the control of mating choices in rodents. Together, the above analyses suggest that, perhaps partly due to excessive production of testosterone and 17β-estradiol, TRPM8$^{-/-}$ males not only exhibit increased aggression[33] (as evidenced in Figure 2A), but also altered sexual preferences[41] (as evidenced in Figure 4C).

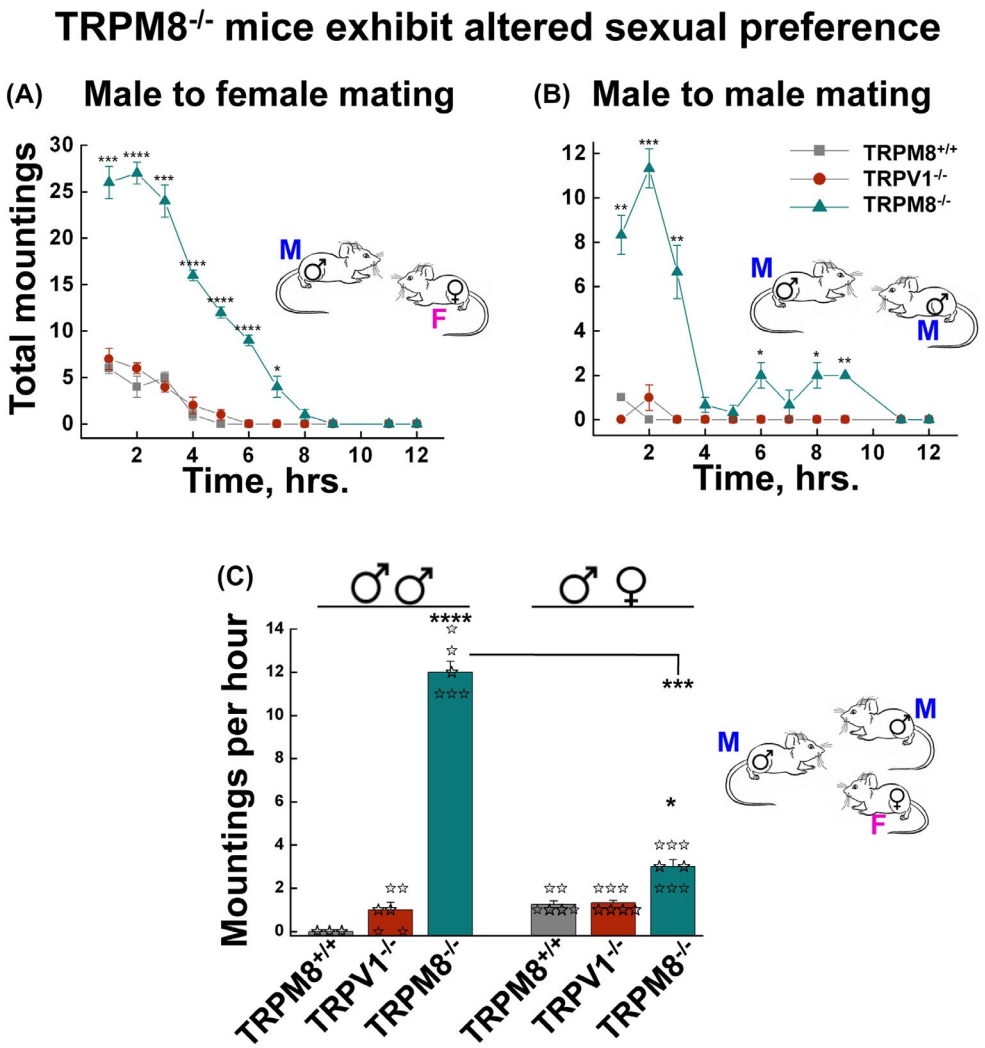

FIGURE 4 TRPM8 knockout mice exhibit enhanced mating behavior and altered sexual preferences. A and B, mounting behavior was assessed for male-female (A) and male-male (B) pairs of the same genotype of mice. Data points represent mean ± s.e.m. of hourly mounting events during the time course of 12 hours following the introduction of the pair, for 8 pairs each of sexually inexperienced TRPM8$^{+/+}$, TRPV1$^{-/-}$, and TRPM8$^{-/-}$ mice performed in eight independent experiments. $^{*}P < .05$, $^{**}P < .01$, $^{***}P < .001$, $^{****}P < .0001$ for TRPM8$^{+/+}$ vs TRPM8$^{-/-}$ of the corresponding time periods. C, TRPM8$^{-/-}$ mice exhibited altered sexual preferences in mating choice test. Two males and one estrous female of the same genotype were placed in the mating cage and the numbers of male-male and male-female mountings during the first 2-hour period were counted. Data are mean ± s.e.m. of at least 10 experiments for each genotype. $P = 3.166 \times 10^{-5}$ for male-male mounting of TRPM8$^{+/+}$ vs TRPM8$^{-/-}$; $P = .036$ for male-female mountings of TRPM8$^{+/+}$ vs TRPM8$^{-/-}$; and $P = 3.85 \times 10^{-4}$ for TRPM8$^{-/-}$ male-male vs male-female mountings. Statistical significance was evaluated using one-way ANOVA test

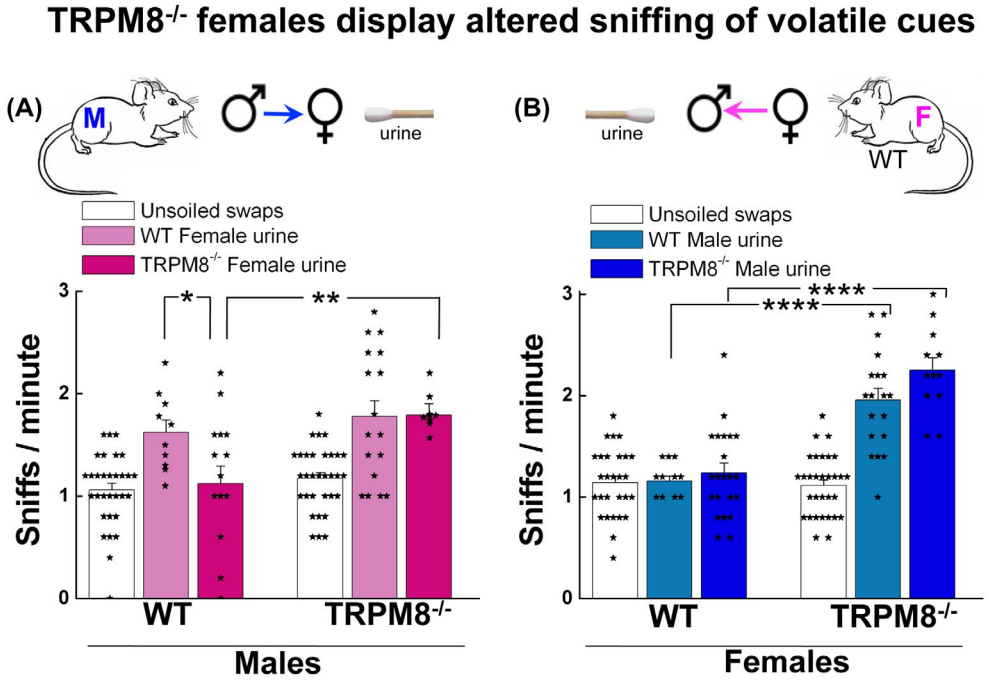

FIGURE 5 TRPM8$^{-/-}$ females display altered sniffing of urine volatile cues. TRPM8$^{+/+}$ and TRPM8$^{-/-}$ mice were exposed to the cotton swabs soaked with urine of the opposite sex of either strain, as illustrated in the scheme above the figures, for 5 minutes and the total number of sniffs was counted and expressed as sniffs per min. A, TRPM8$^{+/+}$ males showed decreased sniffing to urine of TRPM8$^{-/-}$ females compared to urine of TRPM8$^{+/+}$ females ($P = .0443$), while TRPM8$^{-/-}$ males exhibited no preference to urine from TRPM8$^{+/+}$ or TRPM8$^{-/-}$ females ($P = .187$). B, compared to the TRPM8$^{+/+}$, TRPM8$^{-/-}$ females showed a significant increase in sniffing to urine from males of either TRPM8$^{+/+}$ or TRPM8$^{-/-}$ mice ($P = 3.45 \times 10^{-5}$ for TRPM8$^{+/+}$ vs TRPM8$^{-/-}$ female sniffing of TRPM8$^{+/+}$ male urine, and $P = 4.34 \times 10^{-7}$ for TRPM8$^{+/+}$ vs TRPM8$^{-/-}$ female sniffing of TRPM8$^{-/-}$ male urine). Data represent means ± s.e.m for total number of assays indicated inside the bars pooled from six mice in each group. Statistical significance was evaluated using one-way ANOVA test

3.5 | TRPM8 regulates olfaction-exploratory behavior in female animals

Chemosensory input from the olfactory system is a critical stimulus component of mating behavior in rodents.[42,43] The expression of TRPM8 along the olfactory epithelium (OE),[44] olfactory bulb (OB), and the amygdala[45,46] suggests that the channel may play a role in either testosterone-driven olfactory exploration of volatile cues, or transducing testosterone signal from the OE and the OB to the amygdala, as olfactory neurons directly project to this region of the limbic system.[47,48] Here, we further investigated TRPM8 expression along the olfactory-amygdala neural axis. In situ hybridization and immunohistochemistry experiments demonstrated mild expression levels of TRPM8 in the amygdala, particularly in the medial amygdala (MEA) and basolateral amygdala (BLA), where the channel is present in pyramidal neurons (Supporting Figure S6). Conversely, TRPM8 is highly expressed along several layers of the main OB, including mitral, glomerular, and granule layers (Supporting Figures S7 and S8).

Apart from the main olfactory system (MOS), another essential pathway for sensing chemosensory cues and detecting nonvolatile and volatile pheromones is accomplished through the vomeronasal organ (VNO).[49] However, we did not detect any noticeable expression of TRPM8 in the VNO (Supporting Figure S9). Thus, between MOS and VNO, TRPM8 is specifically present in the MOS, a system that plays the dominant role in detecting airborne scents and volatile pheromones.

Testosterone tightly controls the synthesis of pheromones and social behaviors, such as aggressiveness or territoriality, are regularly associated with testosterone-dependent volatiles in urine.[49,50] We reasoned that the elevation of serum testosterone levels in TRPM8$^{-/-}$ mice might further impact the concentrations of pheromones, and in turn the mating behavior, from the chemosensory inputs. Therefore, we tested behaviors of TRPM8$^{-/-}$ mice in olfaction exploration using the volatile sensory cues-dependent sniffing assay, in which the animal was exposed to swabs soaked with urines from TRPM8$^{-/-}$ or WT mice, and the number of sniffs was recorded.

Intriguingly, while TRPM8$^{-/-}$ males were indiscriminate in olfactory exploration toward urines from TRPM8$^{-/-}$ and TRPM8$^{+/+}$ females (Figure 5A), TRPM8$^{+/+}$ males demonstrated increased sniffs exploring urine from the WT females, but not that from TRPM8$^{-/-}$ females, as compared to the unsoiled swabs (Figure 5A). Interestingly, however, while TRPM8$^{+/+}$ males similarly explored urines from TRPM8$^{+/+}$

and TRPM8$^{+/-}$ females, the heterozygous males only exhibited interest to urine from WT, but not TRPM8$^{+/-}$ females (Supporting Figure S10A). Moreover, TRPM8$^{-/-}$ females showed markedly increased sniffs toward urine from males of both TRPM8$^{-/-}$ and TRPM8$^{+/+}$ strains (Figure 5B), in sharp contrast to the general lack of olfactory exploration of TRPM8$^{+/+}$ and TRPM8$^{+/-}$ females (Figure 5B, Supporting Figure S10B). Thus, contrary to the sexual dimorphism in olfactory exploration displayed by the sexually inexperienced WT and heterozygous mice, in which only males showed exploratory behavior toward urine of females, both sexually inexperienced TRPM8$^{-/-}$ males and females exhibited high levels of olfactory explorations to urine from opposite sexes, with the females displaying even somewhat higher activities than males (Figure 5A,B). The finding that the WT males showed interests in urine from WT and TRPM8$^{+/-}$, but not TRPM8$^{-/-}$, females may suggest altered levels or composition of pheromones from TRPM8$^{-/-}$ females, as a result of their altered steroid milieu (Supporting Figure S2). However, the TRPM8$^{-/-}$ males did not display a preference between volatile cues from the WT and TRPM8$^{-/-}$ females, but clearly showed more interests toward urine samples than unsoiled swabs (Figure 5A), indicating that the mutant animals were attracted to pheromone-unrelated substances in the urine. The finding that TRPM8$^{-/-}$ females had similar, or even higher, exploratory activities than TRPM8$^{-/-}$ males further argues for a pheromone-independent cue(s) that drives the olfaction exploration behaviors of the TRPM8$^{-/-}$ mice.

3.6 | Testosterone-induced neural signaling in the brain is attenuated in TRPM8$^{-/-}$ males but not females

The above results suggested that TRPM8 might regulate the reward response to chemosensory cues and the altered behavioral phenotypes of TRPM8$^{-/-}$ mice could result from (a) the increased steroid milieu that enhances activity of genomic receptor pathways (*via* AR or ERs), (b) a diminished testosterone-induced signaling of TRPM8 itself, leading to diminished dopamine release, or (c) both mechanisms. To address the second possibility, we examined the acute effect of testosterone on brain neurons of the WT control and TRPM8$^{-/-}$ mice. In these experiments, we tested the amygdala, an important region of the limbic system that regulates sexual and social behaviors.

Remarkably, measurements of acute testosterone-induced neural activity, assessed by Ca^{2+} imaging of neurons in the MEA nuclei in mouse brain slices, revealed increases in Ca^{2+} signaling in response to 10 nM testosterone in slices prepared from all animals, regardless of the sexes and the genotypes (Figure 6A,B). The response subsided after about 3 minutes. In these experimental settings, the application of vehicle alone (0.0001% ethanol in aCSF) also elicited some background responses. This might be due to the sensitivity of neurons to subtle differences in temperature or ionic composition, and/or mechanical disturbances of the vehicle application. More interestingly, whereas neurons from the WT males yielded markedly higher responses to exogenously applied testosterone than to the vehicle, those from TRPM8$^{-/-}$ males did not show differences in the response to testosterone and the vehicle control, demonstrating a TRPM8-dependent response to the steroid hormone in the amygdala neurons (Figure 6A,C).In contrast, samples from female animals exhibited greater response magnitudes to testosterone than to the vehicle control, but no significant difference between the two genotypes (Figure 6B,C). These changes were evident in both the range of the responses and the proportion of activated cells (Figure 6C,D). Thus, the responses to the exogenously applied testosterone have at least two components: a general one that is detectable mainly in females and independent of TRPM8, and a male-specific one that is dependent on TRPM8. Given that the general response to testosterone is intact in neurons of TRPM8$^{-/-}$ females, it probably reflects activities of other receptor pathways that do not directly require TRPM8 function. Nonetheless, the elevation of the circulating testosterone levels in the TRPM8$^{-/-}$ mice may cause enhanced neuronal activities in vivo, which could underlie the increased olfactory exploration of the mutant animals as shown in Figure 5. More importantly, neurons from WT males displayed an increased response to testosterone, which was significantly diminished in the absence of TRPM8 in males and not present in females of either genotype (Figure 6A-D), demonstrating that apart from the other receptor pathways, TRPM8 mediates a male-specific response to testosterone in amygdala neurons. It is plausible that the loss of such a sex- and TRPM8-dependent testosterone-induced neuronal activity underlies the behavioral phenotype of the TRPM8$^{-/-}$ male mice documented in Figures 1, 2 and 4.

3.7 | Postmating activation of dopaminergic neurons is impaired in TRPM8$^{-/-}$ males

The delayed sexual satiety exhibited by TRPM8$^{-/-}$ mice (Figure 1) and the diminished responsiveness to testosterone obtained from the brain slices of TRMP8$^{-/-}$ males (Figure 6) suggest that TRPM8 may play a critical role in transducing testosterone signal from the amygdala to the mesolimbic system during mating. The altered sexual behaviors found in TRPM8$^{-/-}$ animals are consistent with impairment in reward feedback to mating, which typically involves the dopamine (DA) system of the ventral tegmental area (VTA), a critical component of the mesolimbic pathway in sex reward mechanism.[3,51] Sexual behavior leads to the activation of dopaminergic neurons in the VTA,[52] which receive monosynaptic

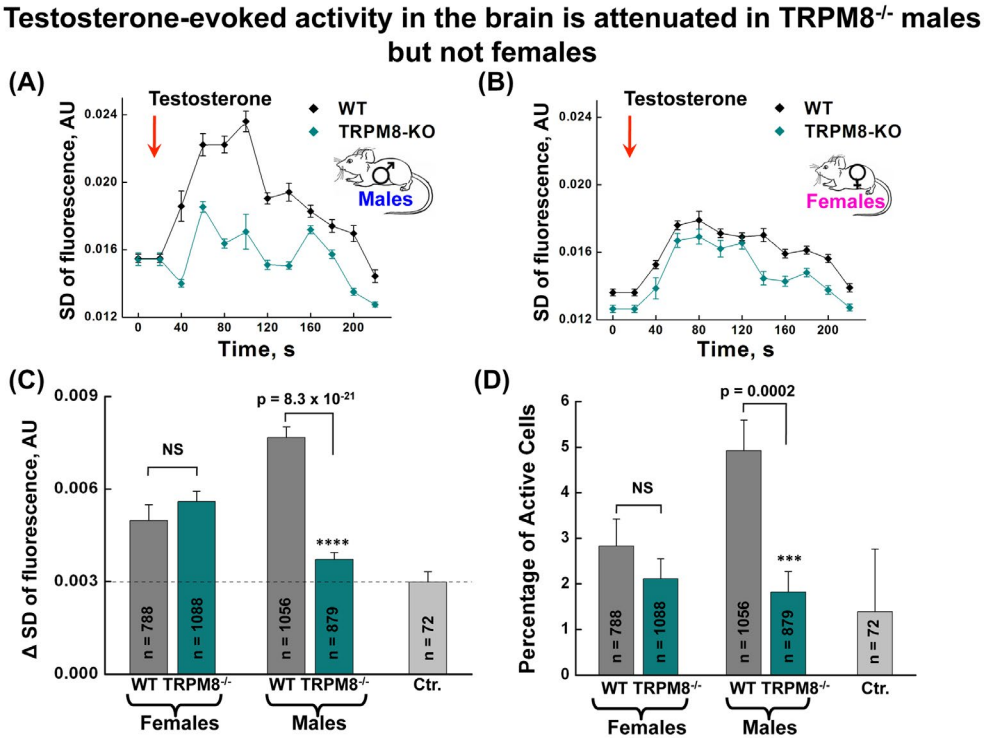

FIGURE 6 Testosterone-induced neural signaling in the brain is attenuated in TRPM8$^{-/-}$ males but not females. A and B, time courses of neuronal activities, assessed as standard deviation of calcium signals, in response to testosterone application (10 nM) along the medial amygdala nuclei in brain slices obtained from the WT and TRPM8$^{-/-}$ male (A) and female (B) mice. C, changes in activity of amygdala cells, expressed as the difference in the standard deviation of the calcium responses during the analysis period (the 200 frames starting at 60 s after testosterone or vehicle application) vs baseline period (the 200 frames just prior to testosterone or vehicle application). A total of 1 mL testosterone solution (diluted from the ethanol stock solution, resulting in the final concentration of 0.0001%), or vehicle (aCSF, containing an equivalent ethanol concentration, 0.0001%) was injected over the course of 2 minutes 10 seconds, bringing the final concentration of testosterone in the perfusion chamber to 10 nM. At 1 minute 40 seconds of the application, which is approximately the time needed for more than a third of the solution to reach the perfusion chamber, imaging was initiated to acquire 2000 frames within 200 seconds. Statistical significance was determined with Student's *t* test. $P = .315$ for WT vs TRPM8$^{-/-}$ females, whereas $P = 8.26 \times 10^{-21}$ for WT vs TRPM8$^{-/-}$ males. The dashed line represents a mean of background response obtained during application of vehicle alone, which contained aCSF and 0.0001% ethanol. All groups except TRPM8$^{-/-}$ males showed significantly greater magnitude responses than vehicle controls (Female WT vs vehicle, $P = .001$, Female TRPM8$^{-/-}$ vs vehicle $P = 1.04 \times 19^{-07}$, Male WT vs vehicle $P = 1.22 \times 10^{-19}$, Male TRPM8$^{-/-}$ vs vehicle $P = .0673$). D, percentage of amygdala cells activated after testosterone or vehicle application. Cells were classified as being activated if their activity during the analysis period exceeded 2.5X the standard deviation of the baseline period. Statistical significance was determined with Chi-Square test. See Methods for details. $P = .322$ for WT vs TRPM8$^{-/-}$ females; $P = .0002$ for WT vs TRPM8$^{-/-}$ males. Error bars correspond to s.e.m for n, number of pooled cells across slices. Four slices were used per animal, with a total of three animals (12 slices) for each group used for testosterone treatment. One WT male mouse was used for vehicle (Ctr.) application

projections directly from the amygdala [53] and subsequently release dopamine in the nucleus accumbens (NAc).[54,55] We hypothesized that activation of TRPM8 by testosterone in the amygdala causes excitatory transmissions to the VTA, which further impacts dopamine release in the NAc. This represents the main pathway of endogenous reward mechanism[52] or drug-induced reinforcement,[56] known to impact sexual experience.[51] To test this hypothesis, we assessed activation of DA neurons before and immediately after mating events of age-matched TRPM8$^{+/+}$ and TRPM8$^{-/-}$ littermates using cFos as a marker of neuron activation.[57] As anticipated, postmating DA neuron activity in the VTA was increased in the TRPM8$^{+/+}$ males, but this was completely abolished in TRPM8$^{-/-}$ males (Figure 7). TRPM8$^{-/-}$ females, moreover, displayed a significant decrease in DA activity when compared to themselves before and post mating; however, no significant difference was detected between TRPM8$^{+/+}$ and TRPM8$^{-/-}$ females either before or after mating. These data clearly show a defect of mating-related reward mechanism in TRPM8$^{-/-}$ males and implicate the VTA DA system as one of the brain loci for sexual dimorphism[58] regulated by TRPM8.

Along with the VTA, we also screened mating-related activation of dopaminergic neurons in several other brain

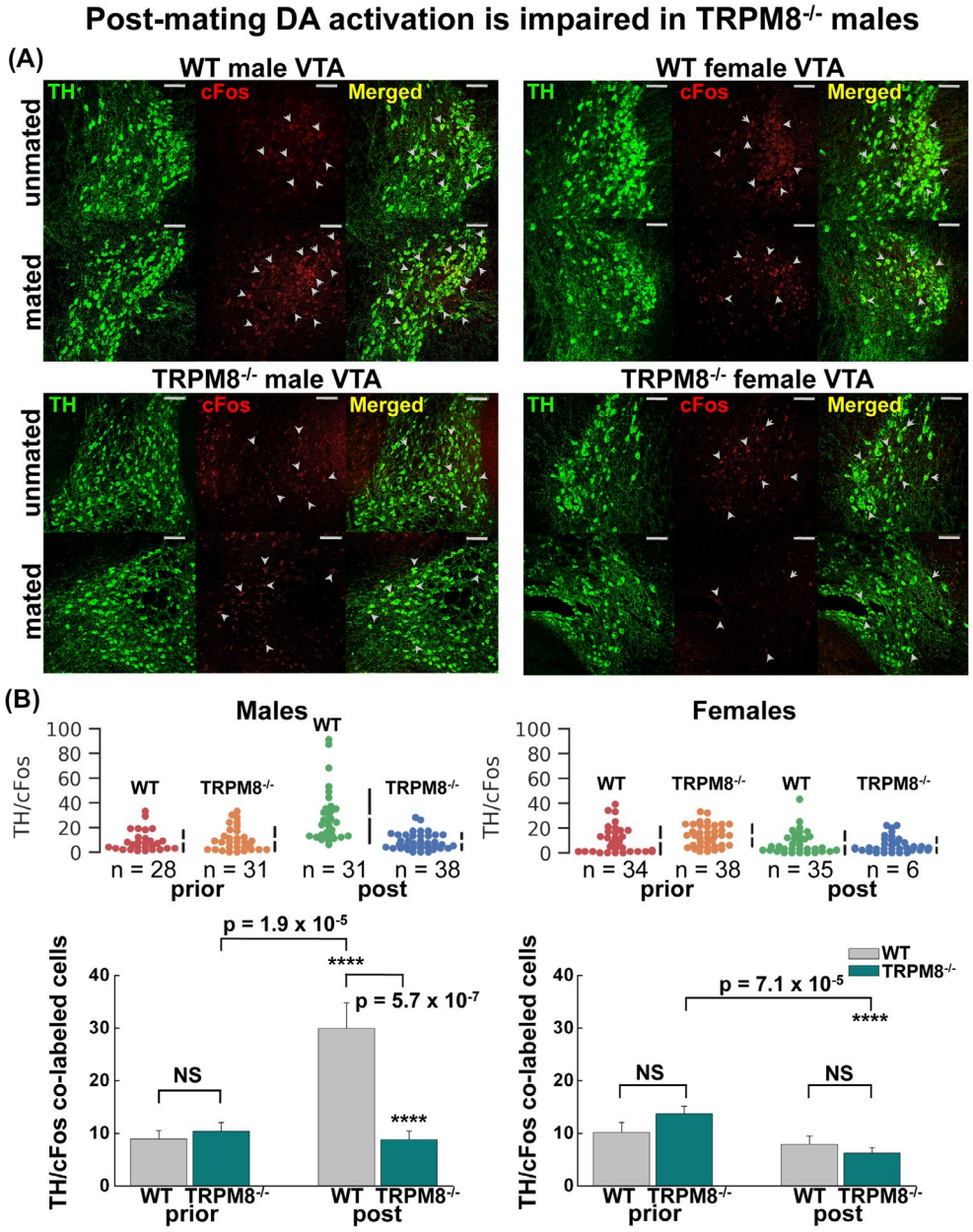

FIGURE 7 TRPM8 mediates sex reward mechanism. Age-matched WT and TRPM8$^{-/-}$ male and female mice were sacrificed before and immediately after mating events and the brains processed for the DA activity by assessing the number of neurons in the VTA co-labeled for DA-specific marker TH and a marker of neuronal activity cFos. A, representative images of TH (green, by Alexa-488) and cFos (red, by Alexa-594) labeled neurons at the VTA regions of coronal brain slices, obtained by confocal microscopy at 20X magnification. Scale bars: 100 μm. B, quantification of the TH/cFos co-labeled cells in VTA before and after mating for the WT and TRPM8$^{-/-}$ male (left panels) and female (right panels) mice for individual slices (upper panels) and mean ± s.e.m (lower panels). Statistical significance was determined using one-way ANOVA test. $P = .537$ for WT vs TRPM8$^{-/-}$ males premating; $P = 1.875 \times 10^{-5}$ for WT males pre- vs post-mating; $P = .423$ for TRPM8$^{-/-}$ males pre- vs post-mating; $P = 5.695 \times 10^{-7}$ for WT vs TRPM8$^{-/-}$ males post-mating; $P = .134$ for WT vs TRPM8$^{-/-}$ females premating; $P = .357$ for WT females pre- vs post-mating; $P = 7.1 \times 10^{-5}$ for TRPM8$^{-/-}$ females pre- vs post-mating; $P = .372$ for WT vs TRPM8$^{-/-}$ females post-mating

regions, including the third ventricle of hypothalamus, arcuate nucleus of hypothalamus, and substantia nigra. However, we found no systemic changes in the activation patterns of DA neurons in these areas of both the TRPM8$^{+/+}$ or TRPM8$^{-/-}$ mice (data not shown), further implying the specificity of this neural circuitry to dopaminergic neurons of the mesolimbic system.

4 | DISCUSSION

Here we present the first evidence linking rapid testosterone signaling component TRPM8 to testosterone-dependent social and sexual behaviors in mice. Importantly, TRPM8 appears to play a different role in sexual behaviors from the canonical AR. A previous study reported that mice lacking AR in the nervous

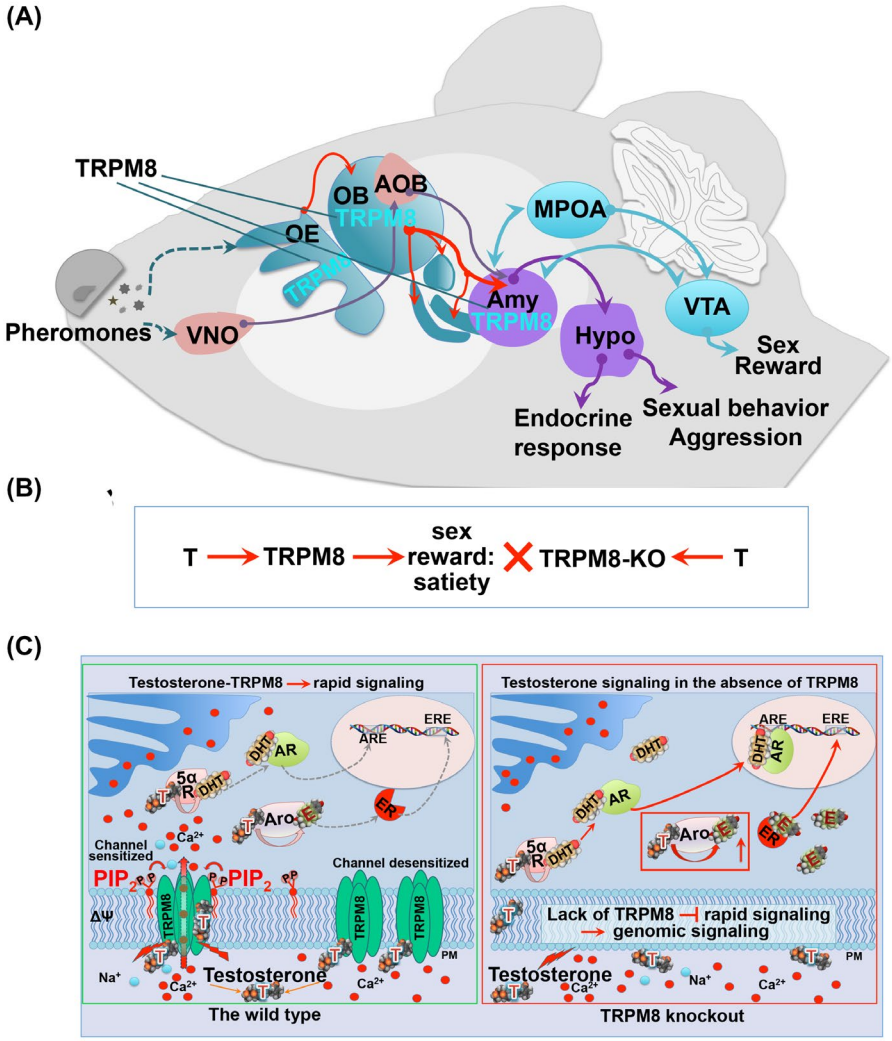

FIGURE 8 TRPM8 expression along the olfactory-amygdala pathway and testosterone-dependent TRPM8 signaling in the wild type and TRPM8$^{-/-}$ mice. A, schematic representation of TRPM8 expression in the olfactory epithelium (OE), olfactory bulb (OB), and the amygdala (Amy). Abbreviations: medial preoptic area (MPOA); ventral tegmental area (VTA); vomeronasal organ (VNO); accessory olfactory bulb (AOB); hypothalamus (Hypo). B, a proposed model for the role of TRPM8 in testosterone (T)-induced reward mechanism, which is diminished in TRPM8$^{-/-}$ (TRPM8-KO), leading to a delayed sexual satiety. C, molecular models of testosterone-dependent signaling in the WT (left) and TRPM8$^{-/-}$ (right) mice. In the WT mice, testosterone-induced TRPM8 activity results in rapid Ca^{2+} or Na^{+} influx. PIP_2 regulates this activity as the prime TRPM8 gating co-factor with all its known agonists. In addition, testosterone (T) taken up by the cell is converted to dihydrotestosterone (DHT) by 5α-reductase (5αR) and estradiol (E) by aromatase (Aro). DHT can bind to the transcription factor Androgen Receptor (AR), with subsequent activation of the target genes at the Androgen Receptor Elements (ARE). E can bind to its cognate receptors, Estrogen Receptors (ER), and regulate their target genes *via* interacting with the Estrogen Receptor Elements (ERE). In TRPM8 knockout mice (right panel), the lack of functional TRPM8 results in diminished rapid testosterone signaling and enhanced levels of testosterone as well as its metabolic products DHT and E, leading to enhanced activation of AR and ER at least in some cell populations

system displayed profound deficits in the pattern of sexual behaviors, including significantly decreased mounting frequency.[27] These are in sharp contrast to the behavioral alterations found in TRPM8$^{-/-}$ mice, such as increased mounting frequency, enhanced sexual motivation, and long-duration mounting prevalence. While some of these behavioral alterations could sprout from an enhanced activity of genomic receptors in the absence of the rapid signaling component of testosterone, others might result from a deficient sexual reward mechanism[52] with possible impact on sexual satiation.[32] Our results suggest that TRPM8 plays a critical role in testosterone-mediated reward mechanism (Figure 8A). The disruption of TRPM8 function eliminates the nongenomic signaling evoked by testosterone that normally occurs through monosynaptic projections from the amygdala to the DA system in the VTA to elicit the reward aspects of sexual behaviors (Figure 8B). As a result, TRPM8$^{-/-}$ mice attempt to compensate this deficiency by increased mating and aggression in males, and enhanced system production of testosterone, which leads to other behavioral changes, such as olfactory exploration in both males and females.

The male-like chemosensory exploratory activity displayed by TRPM8$^{-/-}$ females could also implicate a general impairment of the reward mechanism, which dampens the satisfaction of olfactory stimulation and thereby leading to increased sniffing. Previously, chemosensory cues from conspecifics have been shown to cause dopamine release in the medial preoptic area (MPOA) of the brain, which underlies the reward input from olfactory exploration.[3] Moreover, bilateral removal of the olfactory bulbs eliminated sexual activity and MPOA dopamine release.[59]

Dissecting whether the altered behaviors observed on TRPM8$^{-/-}$ mice are attributed to the increased levels of steroids or lack of testosterone-evoked TRPM8 signaling will require further detailed exploration. However, the present findings suggest that both mechanisms are intertwined. While the enhanced aggressive behavior of TRPM8$^{-/-}$ is most likely driven *via* the implication of ERα, the alteration in DA neuronal activation is unlikely to be attributed to higher levels of testosterone and, thus, to the action of the genomic receptors. Earlier studies demonstrated that in male rats, gonadal steroids regulate basal DA release[31] and stimulate mating.[60] During copulation, the release of DA increases by more than 50%, and this effect requires androgens.[31,60] This process reflects neural reward pathways of sexual behaviors, which involve the mesolimbic DA circuit consisting of VTA and NAc. In rats, DA is released into NAc during sex, where testosterone affects the release of DA through its enhancement of sexual behaviors.[54] Furthermore, in castrated males that do not mate, DA release does not increase.[60] Thus, if higher levels of testosterone would stimulate mating in TRPM8$^{-/-}$ mice, then they would also demonstrate higher levels/activity of DA neurons. However, we observe exactly the contrary. As shown in Figure 7, the levels of activated dopaminergic neurons in TRPM8$^{-/-}$ males do not change after mating. The most plausible explanation to this effect is a deficient neural signal transduction in VTA DA neurons of TRPM8$^{-/-}$ males, and as a result diminished sexual satiety.

Furthermore, this study demonstrates a distinctive role of TRPM8 as an immediate/direct testosterone receptor on behaviors from the classical genomic receptors that regulate these behaviors indirectly through activation or suppression of the downstream target genes.[5] It is conceivable that these findings will boost new investigations on testosterone-TRPM8 signaling in other animal models, and particularly, in humans. Despite the fundamental importance of sexual activities in human life, the neurological control of this behavior is poorly understood and limited to human lesion research, reflecting pathological cases,[61] or neuroimaging techniques assessing this system in healthy individuals.[62] Human lesion research examines the effects of neurological insult on sexual behavior and sexual changes associated with neurological disease, cerebral injury, or neurosurgery.[61] It was shown that impaired functionality of the brain regions responsible for mediation of sexual behavior in humans (eg, the limbic system/amygdala/hypothalamus) could lead to significant alterations, such as disinhibited sexual behavior or various forms of hyper-sexuality.[61,63,64]

Another analogy refers to the Klüver-Bucy syndrome, originally described in primates after the bilateral removal of the anterior temporal lobes. The Klüver-Bucy syndrome presents a cluster of intriguing behavioral changes, among which is hyper-sexuality that is often expressed indiscriminately with absence of fear or expression of anger.[65] In humans, the syndrome has been diagnosed after bilateral temporal damage.[66] Psychopharmacologic studies in primates suggest that lesions disconnecting excitatory projections to the amygdala cause reduced dopamine and serotonin levels and increased norepinephrine levels in the amygdala.[67] In light of these chronicles, our results showing enhanced sexual drive and indiscriminate mountings of TRPM8-deficient mice resemble the hypersexual phenotype observed in primates and humans with limbic system dysfunction,[61,63,64] which most likely sprouts from diminished reward feedback.

Notably, in its distinctive role as an immediate, rapid-signaling testosterone receptor,[7,8] and the behavioral phenotype displayed by the mutant animals, TRPM8 stands apart from other sexually dimorphic genes and classical steroid receptors.[68] A few genes encoding proteins implicated in dimorphic sexual behaviors, when deleted, resulted in either insignificant changes or deficits of mating behaviors,[68] similar to that of the classical AR.[27] To this end, the hypersexual and aggressive phenotypes exhibited by the TRPM8$^{-/-}$ mice implicate a unique role of this channel in regulating testosterone-elicited behaviors.

Moreover, mutant mice deficient in TRPC2 channels exhibit increased activities in mating other males,[69] similar to what we observed in TRPM8$^{-/-}$. However, we believe that this regulation by TRPC2 is distinct from that by TRPM8. TRPC2 is expressed in the VNO, where the channel plays a critical role in pheromone sensation,[69,70] while the TRPM8 expression is entirely lacking from this organ, but, in contrast, present in the MOS. Furthermore, the altered sniffing behaviors of TRPM8$^{-/-}$ mice demonstrate that these behaviors are not affected by pheromones, but rather the likely presence of an alternative neural circuitry in regulating them.

In summary, our research findings highlight a novel regulatory role of TRPM8 in dimorphic sexual behaviors that are part of the reproductive repertoire. Future studies of this rapid signaling component of testosterone and the role of TRPM8 in regulating downstream axes of testosterone metabolites, DHT, and estrogen, acting *via* AR and ERs (Figure 2E), will be instrumental for our understanding of key hormonal elements related to development, sex differences, and reproductive function and shed new lights on therapeutic intervention of sexual dysfunctions.

ACKNOWLEDGMENTS

We are grateful to Junling Yang for her immense help with preparation of the brain slices. The research was supported by the National Science Foundation through the grant IOS-1922428 to EZ; and the National Institutes of Health NIGMS grant award number 1P20GM103432-01 project 4 to BT.

CONFLICT OF INTEREST

The authors declare no conflicts of interest.

AUTHOR CONTRIBUTIONS

A. Mohandass, V. Krishnan, E. Gribkova, S. Asuthkar, P. Baskaran, Y. Nersesyan, and Z. Hussain performed research and analyzed data; L. Wise performed research; R. George analyzed data and highlighted clinical relevance of the study, N. Stokes analyzed data; B. Alexander provided guidance on behavioral study and data analysis, A. Cohen performed MS experiments and data analysis; E. Pavlov contributed new reagents and analytic tools, discussed and edited the paper; D. Llano designed brain-slices research and data analysis, and edited the paper; M. Zhu contributed to research design and edited the paper, B. Thyagarajan and E. Zakharian designed research, performed experiments, analyzed data, and wrote the paper.

REFERENCES

1. Huhtaniemi I. Endocrine and local control testicular regulation. In: Wass JAH, Stewart PM, eds. *Oxford Textbook of Endocrinology and Diabetes*. Oxford University Press; 2011:1347-1353.
2. Mermelstein PG, Becker JB, Surmeier DJ. Estradiol reduces calcium currents in rat neostriatal neurons via a membrane receptor. *J Neurosci*. 1996;16:595-604.
3. Sato SM, Schulz KM, Sisk CL, Wood RI. Adolescents and androgens, receptors and rewards. *Horm Behav*. 2008;53:647-658.
4. Soma M, Kim J, Kato A, Kawato S. Src kinase dependent rapid non-genomic modulation of hippocampal spinogenesis induced by androgen and estrogen. *Front Neurosci*. 2018;12:282.
5. Foradori CD, Weiser MJ, Handa RJ. Non-genomic actions of androgens. *Front Neuroendocrinol*. 2008;29:169-181.
6. Cornil CA, Leung CH, Pletcher ER, Naranjo KC, Blauman SJ, Saldanha CJ. Acute and specific modulation of presynaptic aromatization in the vertebrate brain. *Endocrinology*. 2012;153:2562-2567.
7. Asuthkar S, Elustondo PA, Demirkhanyan L, et al. The TRPM8 protein is a testosterone receptor: I. Biochemical evidence for direct TRPM8-testosterone interactions. *J Biol Chem*. 2015;290:2659-2669.
8. Asuthkar S, Demirkhanyan L, Sun X, et al. The TRPM8 protein is a testosterone receptor: II. functional evidence for an ionotropic effect of testosterone on TRPM8. *J Biol Chem*. 2015;290:2670-2688.
9. Asuthkar S, Velpula KK, Elustondo PA, Demirkhanyan L, Zakharian E. TRPM8 channel as a novel molecular target in androgen-regulated prostate cancer cells. *Oncotarget*. 2015;6:17221-17236.
10. Asuthkar S, Demirkhanyan L, Mueting SR, Cohen A, Zakharian E. High-throughput proteome analysis reveals targeted TRPM8 degradation in prostate cancer. *Oncotarget*. 2017;8:12877-12890.
11. Waddell TG, Jones H, Keith AL. Legendary chemical aphrodisiacs. *J Chem Educ*. 1980;57:341-342.
12. Thompson RJ, Thompson JM, Thompson JR.Methods to treat one or all of the defined etiologies of female sexual dysfunction. *United States Patent Application Publication Pub. No.: US 2005/0245494*; 2005.
13. Byers SL, Wiles MV, Dunn SL, Taft RA. Mouse estrous cycle identification tool and images. *PLoS One*. 2012;7:e35538.
14. Richerson GB, Messer C. Effect of composition of experimental solutions on neuronal survival during rat brain slicing. *Exp Neurol*. 1995;131:133-143.
15. Dong HW. *Allen Reference Atlas: A Digital Color Brain Atlas of the C57Black/6J Male Mouse*. Hoboken, NJ: Wiley; 2008.
16. Yuste R, MacLean J, Vogelstein J, Paninski L. Imaging action potentials with calcium indicators. *Cold Spring Harbor Protocols*. 2011;2011(8):pdb.prot5650.
17. Hatanaka Y, Hojo Y, Mukai H, et al. Rapid increase of spines by dihydrotestosterone and testosterone in hippocampal neurons: Dependence on synaptic androgen receptor and kinase networks. *Brain Res*. 2015;1621:121-132.
18. Guo G, Kang L, Geng D, et al. Testosterone modulates structural synaptic plasticity of primary cultured hippocampal neurons through ERK - CREB signalling pathways. *Mol Cell Endocrinol*. 2020;503:110671.
19. Ishihara Y, Fujitani N, Sakurai H, et al. Effects of sex steroid hormones and their metabolites on neuronal injury caused by oxygen-glucose deprivation/reoxygenation in organotypic hippocampal slice cultures. *Steroids*. 2016;113:71-77.
20. Viant MR, Millam JR, Delany ME, Fry DM. Regulation of brain-derived neurotrophic factor messenger RNA levels in avian hypothalamic slice cultures. *Neuroscience*. 2000;99:373-380.
21. Teoderescu D. Time-series decomposition and forecasting. *Int J Control*. 1989;50:1577-1585.
22. Asuthkar S, Velpula KK, Nalla AK, Gogineni VR, Gondi CS, Rao JS. Irradiation-induced angiogenesis is associated with an MMP-9-miR-494-syndecan-1 regulatory loop in medulloblastoma cells. *Oncogene*. 2014;33:1922-1933.
23. Zakharian E, Thyagarajan B, French RJ, Pavlov E, Rohacs T. Inorganic polyphosphate modulates TRPM8 channels. *PLoS One*. 2009;4:e5404.
24. Shevchenko A, Tomas H, Havlis J, Olsen JV, Mann M. In-gel digestion for mass spectrometric characterization of proteins and proteomes. *Nat Protoc*. 2006;1:2856-2860.
25. Zakharian E, Cao C, Rohacs T. Gating of transient receptor potential melastatin 8 (TRPM8) channels activated by cold and chemical agonists in planar lipid bilayers. *J Neurosci*. 2010;30:12526-12534.
26. Zakharian E. Recording of ion channel activity in planar lipid bilayer experiments. *Methods Mol Biol*. 2013;998:109-118.
27. Juntti SA, Tollkuhn J, Wu MV, et al. The androgen receptor governs the execution, but not programming, of male sexual and territorial behaviors. *Neuron*. 2010;66:260-272.
28. Hamson DK, Jones BA, Watson NV. Distribution of androgen receptor immunoreactivity in the brainstem of male rats. *Neuroscience*. 2004;127:797-803.
29. McKemy DD, Neuhausser WM, Julius D. Identification of a cold receptor reveals a general role for TRP channels in thermosensation. *Nature*. 2002;416:52-58.
30. Peier AM, Moqrich A, Hergarden AC, et al. A TRP channel that senses cold stimuli and menthol. *Cell*. 2002;108:705-715.

31. Putnam SK, Sato S, Hull EM. Effects of testosterone metabolites on copulation and medial preoptic dopamine release in castrated male rats. *Horm Behav*. 2003;44:419-426.
32. Rodriguez-Manzo G, Guadarrama-Bazante IL, Morales-Calderon A. Recovery from sexual exhaustion-induced copulatory inhibition and drug hypersensitivity follow a same time course: two expressions of a same process? *Behav Brain Res*. 2011;217:253-260.
33. Ogawa S, Washburn TF, Taylor J, Lubahn DB, Korach KS, Pfaff DW. Modifications of testosterone-dependent behaviors by estrogen receptor-alpha gene disruption in male mice. *Endocrinology*. 1998;139:5058-5069.
34. Honda S, Harada N, Ito S, Takagi Y, Maeda S. Disruption of sexual behavior in male aromatase-deficient mice lacking exons 1 and 2 of the cyp19 gene. *Biochem Biophys Res Commun*. 1998;252:445-449.
35. Toda K, Okada T, Takeda K, et al. Oestrogen at the neonatal stage is critical for the reproductive ability of male mice as revealed by supplementation with 17beta-oestradiol to aromatase gene (Cyp19) knockout mice. *J Endocrinol*. 2001;168:455-463.
36. Toda K, Saibara T, Okada T, Onishi S, Shizuta Y. A loss of aggressive behaviour and its reinstatement by oestrogen in mice lacking the aromatase gene (Cyp19). *J Endocrinol*. 2001;168:217-220.
37. Cao C, Yudin Y, Bikard Y, et al. Polyester modification of the mammalian TRPM8 channel protein: implications for structure and function. *Cell Rep*. 2013;4:302-315.
38. Lyng FM, Jones GR, Rommerts FF. Rapid androgen actions on calcium signaling in rat sertoli cells and two human prostatic cell lines: similar biphasic responses between 1 picomolar and 100 nanomolar concentrations. *Biol Reprod*. 2000;63:736-747.
39. Lynch KS, Crews D, Ryan MJ, Wilczynski W. Hormonal state influences aspects of female mate choice in the Tungara Frog (*Physalaemus pustulosus*). *Horm Behav*. 2006;49:450-457.
40. Schellino R, Trova S, Cimino I, et al. Opposite-sex attraction in male mice requires testosterone-dependent regulation of adult olfactory bulb neurogenesis. *Sci Rep*. 2016;6:36063.
41. Balthazart J. Minireview: hormones and human sexual orientation. *Endocrinology*. 2011;152:2937-2947.
42. Hull EM, Dominguez JM. Sexual behavior in male rodents. *Horm Behav*. 2007;52:45-55.
43. Kelliher KR, Wersinger SR. Olfactory regulation of the sexual behavior and reproductive physiology of the laboratory mouse: effects and neural mechanisms. *Ilar J*. 2009;50:28-42.
44. Morenilla-Palao C, Luis E, Fernandez-Pena C, et al. Ion channel profile of TRPM8 cold receptors reveals a role of TASK-3 potassium channels in thermosensation. *Cell Rep*. 2014;8:1571-1582.
45. Lein ES, Hawrylycz MJ, Ao N, et al. Genome-wide atlas of gene expression in the adult mouse brain. *Nature*. 2007;445:168-176.
46. Ordas P, Hernandez-Ortego P, Vara H, et al. Expression of the cold thermoreceptor TRPM8 in rodent brain thermoregulatory circuits. *J Comp Neurol*. 2019. 1–23. https://doi.org/10.1002/cne.24694
47. Sokolowski K, Corbin JG. Wired for behaviors: from development to function of innate limbic system circuitry. *Front Mol Neurosci*. 2012;5:55.
48. Kevetter GA, Winans SS. Connections of the corticomedial amygdala in the golden hamster. II. Efferents of the "olfactory amygdala". *J Comp Neurol*. 1981;197:99-111.
49. Asaba A, Hattori T, Mogi K, Kikusui T. Sexual attractiveness of male chemicals and vocalizations in mice. *Front Neurosci*. 2014;8:231.
50. Bronson FH. The reproductive ecology of the house mouse. *Q Rev Biol*. 1979;54:265-299.
51. Beloate LN, Omrani A, Adan RA, Webb IC, Coolen LM. Ventral tegmental area dopamine cell activation during male rat sexual behavior regulates neuroplasticity and d-amphetamine cross-sensitization following sex abstinence. *J Neurosci*. 2016;36:9949-9961.
52. Balfour ME, Yu L, Coolen LM. Sexual behavior and sex-associated environmental cues activate the mesolimbic system in male rats. *Neuropsychopharmacology*. 2004;29:718-730.
53. Menegas W, Bergan JF, Ogawa SK, et al. Dopamine neurons projecting to the posterior striatum form an anatomically distinct subclass. *eLife*. 2015;4:e10032.
54. Pfaus JG, Damsma G, Nomikos GG, et al. Sexual behavior enhances central dopamine transmission in the male rat. *Brain Res*. 1990;530:345-348.
55. Damsma G, Pfaus JG, Wenkstern D, Phillips AG, Fibiger HC. Sexual behavior increases dopamine transmission in the nucleus accumbens and striatum of male rats: comparison with novelty and locomotion. *Behav Neurosci*. 1992;106:181-191.
56. Corre J, van Zessen R, Loureiro M, et al. Dopamine neurons projecting to medial shell of the nucleus accumbens drive heroin reinforcement. *eLife*. 2018;7:e39945.
57. Bullitt E. Expression of c-fos-like protein as a marker for neuronal activity following noxious stimulation in the rat. *J Comp Neurol*. 1990;296:517-530.
58. Gillies GE, Virdee K, McArthur S, Dalley JW. Sex-dependent diversity in ventral tegmental dopaminergic neurons and developmental programing: a molecular, cellular and behavioral analysis. *Neuroscience*. 2014;282:69-85.
59. Triemstra JL, Nagatani S, Wood RI. Chemosensory cues are essential for mating-induced dopamine release in MPOA of male Syrian hamsters. *Neuropsychopharmacology*. 2005;30:1436-1442.
60. Hull EM, Du J, Lorrain DS, Matuszewich L. Extracellular dopamine in the medial preoptic area: implications for sexual motivation and hormonal control of copulation. *J Neurosci*. 1995;15:7465-7471.
61. Baird AD, Wilson SJ, Bladin PF, Saling MM, Reutens DC. Neurological control of human sexual behaviour: insights from lesion studies. *J Neurol Neurosurg Psychiatry*. 2007;78:1042-1049.
62. Stoleru S, Fonteille V, Cornelis C, Joyal C, Moulier V. Functional neuroimaging studies of sexual arousal and orgasm in healthy men and women: a review and meta-analysis. *Neurosci Biobehav Rev*. 2012;36:1481-1509.
63. Ferretti A, Caulo M, Del Gratta C, et al. Dynamics of male sexual arousal: distinct components of brain activation revealed by fMRI. *NeuroImage*. 2005;26:1086-1096.
64. Gorman DG, Cummings JL. Hypersexuality following septal injury. *Arch Neurol*. 1992;49:308-310.
65. Kluver H, Bucy PC. Preliminary analysis of functions of the temporal lobes in monkeys. 1939. *J Neuropsychiatry Clin Neurosci*. 1997;9:606-620.
66. Terzian H, Ore GD. Syndrome of Kluver and Bucy; reproduced in man by bilateral removal of the temporal lobes. *Neurology*. 1955;5:373-380.
67. Kling AS, Tachiki K, Lloyd R. Neurochemical correlates of the Kluver-Bucy syndrome by in vivo microdialysis in monkey. *Behav Brain Res*. 1993;56:161-170.
68. Xu X, Coats JK, Yang CF, et al. Modular genetic control of sexually dimorphic behaviors. *Cell*. 2012;148:596-607.

69. Leypold BG, Yu CR, Leinders-Zufall T, Kim MM, Zufall F, Axel R. Altered sexual and social behaviors in trp2 mutant mice. *Proc Natl Acad Sci U S A*. 2002;99:6376-6381.
70. Stowers L, Holy TE, Meister M, Dulac C, Koentges G. Loss of sex discrimination and male-male aggression in mice deficient for TRP2. *Science*. 2002;295:1493-1500.

SUPPORTING INFORMATION

Additional Supporting Information may be found online in the Supporting Information section.

How to cite this article: Mohandass A, Krishnan V, Gribkova ED, et al. TRPM8 as the rapid testosterone signaling receptor: Implications in the regulation of dimorphic sexual and social behaviors. *The FASEB Journal*. 2020;34:10887–10906. https://doi.org/10.1096/fj.202000794R